Molybdenum Catalyzed Ammonia Borane Dehydrogenation: Oxidation State Specific Mechanisms

Joshua A. Buss, Guy A. Edouard, Christine Cheng, Jade Shi, and Theodor Agapie*

Division of Chemistry and Chemical Engineering, California Institute of Technology, 1200 East California Boulevard, MC 127-72, Pasadena, California 91125, United States

Supporting Information

Contents

Experimental Details

General Considerations

Unless otherwise specified, all operations were carried out in an MBraun drybox under a nitrogen atmosphere or using standard Schlenk and vacuum line techniques. Solvents for air- and moisture-sensitive reactions were dried over sodium benzophenone ketyl, calcium hydride, or by the method of Grubbs.[1] Deuterated solvents were purchased from Cambridge Isotope Laboratories and vacuum transferred from sodium benzophenone ketyl (C_6D_6) or calcium hydride (CD_3CN and CD_2Cl_2). All solvents, once dried and degassed, were stored under inert atmosphere over 4 Å molecular sieves. Ammonia borane and all amino-borane analogs were sublimed prior to use and stored at -35 °C unless noted otherwise. Magnesium turnings were oven dried prior to use. All other compounds were used as received. Diphosphine **1**,[2] $Mo(CO)_3(MeCN)_3$,[3] **9**,[4] **10**,[5] **11**,[6] ND_3BH_3, NH_3BD_3, ND_3BD_3[7] and NH_3BEt_3[8] were prepared and purified according to literature procedures. $Mo(CO)_6$ was purchased from Strem Chemicals, Inc. Diethylene glycol dimethyl ether (diglyme) was purchased from TCI America. Silver trifluoromethanesulfonate (triflate) was purchased from Alfa Aesar. Magnesium turnings were purchased from Fischer Scientific. Ammonia borane, $LiHBEt_3$ (Superhydride), sodium tetraphenyl borate, dimethylamine borane, and trimethylamine borane were all purchased from Sigma Aldrich. H_2 and D_2 gases were purchased from American Air Liquide and Cambridge Isotope Laboratories, respectively. HD was prepared according to a previously reported procedure[9] and purified via passage through a -196 °C cold trap prior to use. ^1H, ^{13}C, and ^{31}P NMR spectra were recorded on Varian Mercury 300 MHz, Varian 400 MHz, or Varian INOVA-500 spectrometers with shifts reported in parts per million (ppm). ^{11}B NMR spectra were recorded for samples prepared in quartz NMR tubes, using a Varian 400 MHz spectrometer equipped with a quartz probe insert. ^1H and $^{13}C\{^1H\}$ NMR spectra are referenced to residual solvent peaks.[10] ^{31}P and ^{11}B chemical shifts are referenced to external 85% H_3PO_4 (0 ppm) and $NaBPh_4$ (-7.26 ppm) standards, respectively. IR spectra were obtained as solution samples using a CaF_2 window cell on a Thermo Scientific Nicolet 6700 FT-IR spectrometer. Photolyses were conducted using an Oriel Instruments arc lamp housing and a Newport Corporation 200 W Hg/Xe arc lamp set to a current of 8 A. During irradiation, samples were cooled with a dry ice/acetone bath. Elemental analysis was conducted by Robertson Microlit Laboratories, Inc. (Ledgewood, NJ).

*Synthesis of **2***

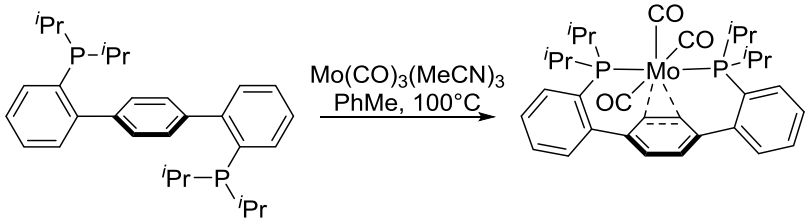

1 **2**

Addition of $Mo(CO)_3(MeCN)_3$ (1.43 g, 4.75 mmol) to a clear solution of **1** (2.05 g, 4.32 mmol) in toluene (50 mL) resulted in a yellow/green heterogeneous mixture. Following heating to 100 °C and stirring for 12 h, the mixture became a deep orange homogenous solution. The volatiles were removed *in vacuo*. The resulting orange solids were collected and washed with cold hexanes (2 x 15 mL). Residual volatiles were removed under reduced pressure to yield **2** (2.54 g, 3.81 mmol, 88 %). X-ray quality crystals were grown from vapor diffusion of pentane into a saturated THF solution of **2**. ^1H NMR (500 MHz, CD_2Cl_2, 25 °C) δ: 7.86 (m, 2H, aryl-*H*), 7.53 (m, 6H, aryl-*H*), 6.52 (br s, 4H, central arene-*H*), 2.75 (br s, 4H, C*H*$(CH_3)_2$), and 1.09-1.23 (br s, 24H, CH(C*H*$_3)_2$). $^{13}C\{^1H\}$ NMR (101 MHz, CD_2Cl_2, 25 °C) δ: 221.15 (t, J = 10.19 Hz, Mo-*C*O), 213.75 (t, J = 8.87 Hz, Mo-*C*O), 148.80 (t, J = 6.90 Hz, aryl-*C*), 139.99 (t, J = 2.74, central arene-*C*), 131.23 (s, aryl-*C*H), 131.02 (t, J = 9.41 Hz, aryl-*C*), 129.90 (s, aryl-*C*H), 129.35 (s, aryl-*C*H), 128.34 (s, aryl-*C*H), 33.83 (br s, *C*H$(CH_3)_2$), 19.88 (s, CH(*C*H$_3)_2$), and 19.43 (s, CH(*C*H$_3)_2$). $^{31}P\{^1H\}$

NMR (121 MHz, C_6D_6, 25 °C) δ: 51.01. IR (CaF_2 window, C_6H_6, cm^{-1}) ν_{CO}: 2298.5, 2192.8. Anal. Calcd. for **2** $C_{33}H_{40}MoO_3P_2$ (%): C, 61.68; H, 6.27. Found: C, 61.43; H, 5.99.

*Synthesis of **3***

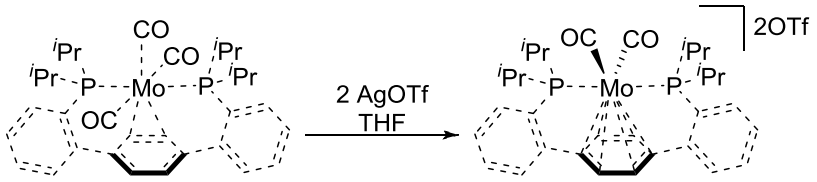

2 **3**

To a rapidly stirring solution of **2** (1.17 g, 1.82 mmol) in THF (50 mL), a solution of AgOTf (1.00 g, 3.83 mmol) in THF (35 mL) was added dropwise. With each drop, an immediate darkening of the solution was observed. Complete addition of the silver solution led to a persistent purple/brown mixture, which was stirred at room temperature for 3 h. The volatiles were removed under reduced pressure to yield green/brown solids. These solids were collected on a fritted glass funnel and washed with THF (3 x 10 mL). The solid residue was extracted into MeCN (30 mL), filtered through Celite, and the resulting yellow solution was dried *in vacuo*. The yellow solids were dissolved in minimal MeCN and filtered through celite once more.[I] Et_2O was added to the filtrate which was then cooled to -35 °C. The precipitate was collected via vacuum filtration, providing **3** (1.16 g, 1.26 mmol, 69 %) as yellow microcrystals. X-ray quality crystals were obtained from vapor diffusion of diethyl ether into a saturated MeCN solution of **3**. ^{1}H NMR (300 MHz, CD_3CN, 25 °C) δ: 7.93 (m, 2H, aryl-*H*), 7.83 (m, 6H, aryl-*H*), 7.15 (s, 4H, central arene-*H*), 3.35 (m, 4H, C*H*$(CH_3)_2$), and 1.29-1.44 (m, 24H, CH(C*H*$_3)_2$). ^{13}C{^{1}H} NMR (101 MHz, CD_3CN, 25 °C) δ: 219.03 (s, Mo-*C*O), 141.32 (dd, *J* = 7.58, 5.79, aryl-*C*), 137.69 (t, *J* = 3.93 Hz, central arene-*C*), 134.64 (s, aryl-*C*H), 133.93 (dd, *J* = 47.74, 8.22, aryl-*C*), 133.83 (s, aryl-*C*H), 132.12 (t, *J* = 3.07 Hz, aryl-*C*H), 128.58 (t, *J* = 5.70 Hz, aryl-*C*H), 122.07 (q, *J* = 320.73 Hz, $F_3CSO_3^-$), 104.72 (s, central arene-*C*H), 28.97 (q, *J* = 11.67 Hz, *C*H$(CH_3)_2$), 18.47 (s, CH(*C*H$_3)_2$), and 18.07 (s, CH(*C*H$_3)_2$). ^{31}P{^{1}H} NMR (121 MHz, CD_3CN, 25 °C) δ: 75.05. IR (CaF_2 window, C_6H_6, cm^{-1}) ν_{CO}: 2025.2, 1986.4. Anal. Calcd. for **3** $C_{34}H_{40}F_6MoO_8P_2S_2$ (%): C, 44.74; H, 4.42. Found: C, 44.65; H, 4.49.

*Synthesis of **4***

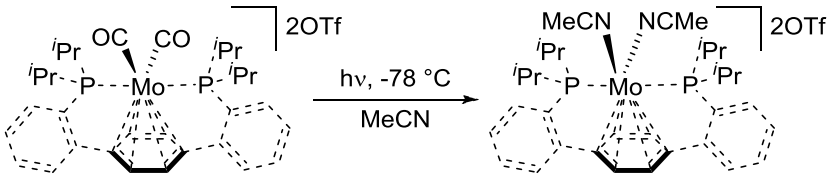

3 **4**

A bright yellow acetonitrile (20 mL) solution of **3** (533 mg, 0.583 mmol) was transferred to a quartz Schlenk tube, charged with a stir bar. The tube was degassed via three freeze-pump-thaw cycles and then, while stirring, irradiated with a 200 W Hg/Xe lamp at -78 °C for 2 h. The evolution of bubbles was observed and the solution steadily darkened to deep red. The flask was degassed as above and photolysis continued. With continued irradiation, the solution darkened to a deep purple color that glowed intensely under the UV light. This degas/irradiation process was continued until aliquots of the solution showed no presence of **3** or the putative monocarbonyl species by ^{31}P NMR (75.05 and 68.62 ppm, respectively). The total irradiation time was dependent on lamp age, frequency of degassing, and solution concentration, varying from 12 h to several days. Upon complete conversion, volatiles were removed under reduced pressure, providing deep purple solids. These solids were collected on a fritted funnel and washed with

[I] Omission of this second filtration step resulted in a less-soluble yellow/orange impurity noticed when employing **3** in the preparation of **4**.

THF until the filtrate was colorless. The purple microcrystalline product was collected (528 mg, 0.565 mmol, 97 %). Crystals suitable for X-ray diffraction were obtained from vapor diffusion of Et_2O into a saturated MeCN solution of **4**. ^{1}H NMR (300 MHz, CD_3CN, 25 °C) δ: 7.62-7.72 (m, 6H, aryl-*H*), 7.51-7.52 (m, 2H, aryl-*H*), 5.59 (t, 4H, *J* = 2.2 Hz, central arene-*H*), 2.86-2.93 (m, 4H, C*H*$(CH_3)_2$), 2.72 (m, 6H, NC(C*H*$_3$)), and 1.25-1.31 (m, 24H, CH(C*H*$_3$)$_2$). ^{13}C{^{1}H} NMR (126 MHz, CD_3CN, 25 °C) δ: 145.36 (t, *J* = 10.51 Hz, aryl-*C*), 143.35 (s, N*C*CH_3), 133.44 (s, aryl-*C*H), 132.35 (s, aryl-*C*H), 130.60 (dd, *J* = 62.25, 23.73, aryl-*C*), 130.57 (s, aryl-*C*H), 127.48 (s, aryl-*C*H), 123.39 (s, Mo- *C*NCH_3), 122.15 (q, *J* = 318.51, $F_3CSO_3^-$), 120.50 (s, central arene-*C*), 88.90 (s, central arene-*C*H), 25.74 (t, *J* = 9.77 Hz, *C*H$(CH_3)_2$), 18.67 (s, CH(*C*H_3)$_2$), 17.86 (s, CH(*C*H_3)$_2$), 7.03 (s, Mo-NC*C*H_3) and 6.52 (m, Mo-NC*C*H_3). ^{31}P{^{1}H} NMR (121 MHz, CD_3CN, 25 °C) δ: 63.35. Anal. Calcd. for **4** $C_{36}H_{46}F_6MoN_2O_6P_2S_2$ (%): C, 46.06; H, 4.94; N, 2.98. Found: C, 45.09; H, 4.77; N, 3.25.

*Synthesis of **5***

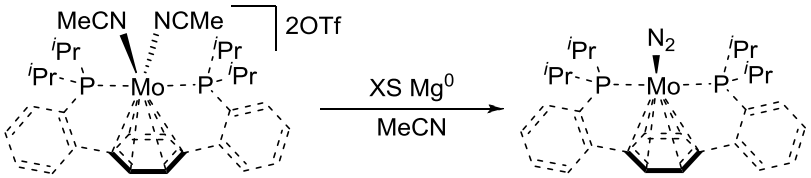

4 **5**

A deep purple solution of **4** (225 mg, 0.241 mmol) in MeCN (4 mL) was portioned into four 20 mL scintillation vials, each charged with a stir bar and an excess of magnesium turnings (3-5 g/vial). The solution was stirred at room temperature for 8 h, during which time it lightened to a green/brown heterogeneous mixture. The mixtures were filtered through celite. Each vial was rinsed with MeCN (2 x 1.5 mL) and each rinse was likewise filtered. The insoluble material was extracted in benzene and dried *in vacuo*, providing a brown/green residue. This residue was extracted with benzene and filtered through celite once more. The brown filtrate solution was lyophilized, yielding **5** as a red/brown powder (108 mg, 0.184 mmol, 76 %). X-ray quality crystals were grown by either vapor diffusion of pentane into a saturated toluene solution of **5** at -35 °C or by chilling a saturated hexanes solution of **5** (-35 °C).

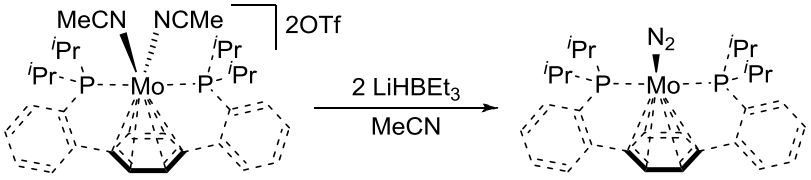

4 **5**

In an alternate synthesis, a 20 mL scintillation vial was charged with **4** (370 mg, 0.396 mmol), MeCN (15 mL), and a stir bar. Stirring was initiated, and 1.0 M $LiHBEt_3$ in THF (0.80 mL, 0.792 mmol) was added to the purple solution dropwise. An immediate color change to reddish-brown was observed. Stirring continued for 12 h, furnishing a green/brown suspension. Volatiles were removed under reduced pressure affording brown solids. The solids were extracted with benzene (10 mL) and filtered. The filtrate was lyophilized, giving **5** as a red/brown powder (63 mg, 0.107 mmol, 27 %). ^{1}H NMR (300 MHz, C_6D_6, 25 °C) δ: 7.48-7.50 (m, 2H, aryl-*H*), 7.23-7.27 (m, 2H, aryl-*H*), 7.02-7.09 (m, 4H, aryl-*H*), 4.26 (s, 2H, central arene-*H*), 3.99 (s, 2H, central arene-*H*), 2.38-2.50 (m, 2H, C*H*$(CH_3)_2$), 2.20-2.31 (m, 2H, C*H*$(CH_3)_2$), and 0.94-1.27 (m, 24H, CH(C*H*$_3$)$_2$). ^{13}C{^{1}H} NMR (101 MHz, C_6D_6, 25 °C) δ: 150.23-150.84 (m, aryl-*C*), 130.50 (s, aryl-*C*H), 128.21 (s, aryl-*C*H), 126.62 (s, aryl-*C*H), 126.06 (s, central arene-*C*), 97.47 (s, central arene-*C*), 82.04 (s, central arene-*C*H), 75.29 (s, central arene-*C*H), 29.71 (br t, *J* = 6.20, *C*H$(CH_3)_2$), 28.17 (br t, *J* = 5.33, *C*H$(CH_3)_2$), 21.14 (br t, *J* = 5.06, CH(*C*H_3)$_2$), 19.85 (br t, *J* = 4.31, CH(*C*H_3)$_2$), 19.59 (s, CH(*C*H_3)$_2$), and 19.16 (s, CH(*C*H_3)$_2$). ^{31}P{^{1}H} NMR (121 MHz, C_6D_6, 25 °C) δ: 76.72. IR (CaF_2 window, C_6H_6, cm^{-1}) $\nu_{N\text{-}N}$: 2020.2. Anal. Calcd. for **5** $C_{30}H_{40}MoN_2P_2$ (%): C, 61.43; H, 6.87; N, 4.78. Found: C, 61.40; H, 6.67; N, 3.68.

*Synthesis of **6***

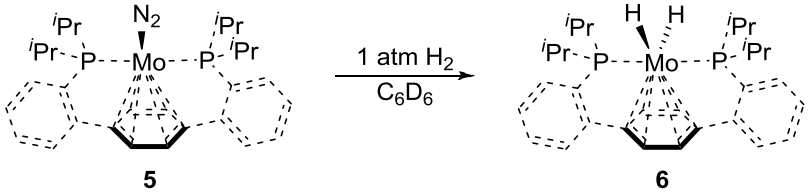

5 **6**

A J. Young NMR tube was charged with a brown/red solution of **5** (20 mg, 0.034 mmol) in C_6D_6 (0.7 mL). The solution was degassed via three freeze-pump-thaw cycles. The headspace was backfilled with H_2 gas, enacting an immediate reddening of the solution. The NMR tube was mechanically rotated for 15 min, providing a red solution of **6**. Isolation and recrystallization of **6** is hampered by its conversion back to **5** in the presence of N_2. ^{1}H NMR (300 MHz, C_6D_6, 25 °C) δ: 7.44-7.48 (m, 2H, aryl-*H*), 6.97-7.11 (m, 6H, aryl-*H*), 4.81 (t, 4H, *J* = 3.17 Hz, central arene-*H*), 2.12-2.24 (m, 4H, C*H*(CH_3)$_2$), 1.23-1.30 (m, 12H, CH(C*H*$_3$)$_2$), 0.92-0.99 (m, 12H, CH(C*H*$_3$)$_2$), and -4.10 (t, 1H, *J* = 35.8 Hz, Mo-*H*). ^{13}C{^{1}H} NMR (126 MHz, C_6D_6, 25 °C) δ: 150.20-150.55 (m, aryl-*C*), 147.38-147.73 (m, aryl-*C*), 128.34 (s, aryl-*C*H), 126.45 (s, aryl-*C*H), 94.38 (s, central arene-*C*), 74.40 (s, central arene-*C*H), 75.29 (s, central arene-*C*H), 30.05 (t, *J* = 9.71, *C*H(CH_3)$_2$), 20.27 (s, CH(*C*H$_3$)$_2$), and 19.49 (s, CH(*C*H$_3$)$_2$). ^{31}P{^{1}H} NMR (121 MHz, C_6D_6, 25 °C) δ: 89.70.

*Synthesis of **6-HD***

The hydride-deuteride isotopolog can be prepared analogously utilizing H–D gas rather than H_2 gas. This gave rise to a 3:5:2 mixture of **6-H$_2$**:**6-HD**:**6-D$_2$**. Integration of the hydridic resonances is omitted. ^{1}H NMR (400 MHz, C_6D_6, 25 °C) δ: 7.45-7.47 (m, 2H, aryl-*H*), 7.16-7.06 (m, 2H, aryl-*H*), 6.96-7.02 (m, 2H, aryl-*H*), 4.81 (br t, 4H, *J* = 2.52 Hz, central arene-*H*), 2.12-2.24 (m, 4H, C*H*(CH_3)$_2$), 1.24-1.30 (m, 12H, CH(C*H*$_3$)$_2$), 0.93-0.98 (m, 12H, CH(C*H*$_3$)$_2$), -4.10 (t, *J* = 33.9 Hz, **6-H$_2$** Mo-*H*), -4.12 (tt, J_{HD} = 10.8 Hz, J_{HP} = 34.0 Hz, **6-HD** Mo-*H*). ^{31}P{^{1}H} NMR (162 MHz, C_6D_6, 25 °C) δ: 89.70 (s, **6-H$_2$**), 89.44 (t, J_{DP} = 4.3 Hz, **6-HD**), and 89.04 (q, J_{DP} = 4.4 Hz, **6-D$_2$**).

*Synthesis of **7***

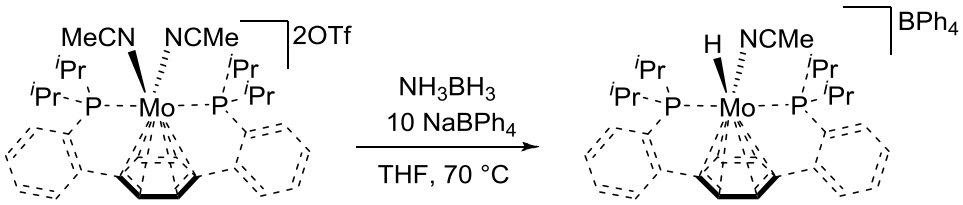

4 **7**

To a Schlenk tube charged with **4** (142 mg, 0.152 mmol), $NaBPh_4$ (107 mg, 0.313 mmol), and a stir bar, a THF (7 mL) solution of AB (5.0 mg, 0.162 mmol) in was added. The purple/brown suspension was heated to 70 °C with stirring for 4 h, providing a homogeneous orange solution. Volatiles were removed *in vacuo*, furnishing an orange powder. DCM (3 mL) was added and the powder was filtered through a Celite plug. Volatiles were again removed and the resulting residue was crystallized via pentane vapor diffusion into a concentrated THF solution. Generally additional recrystallizations were conducted to fully remove the B-N reaction byproducts, providing pure **7** as X-ray quality red/orange blades (89 mg, 0.097 mmol, 64 %). ^{1}H NMR (400 MHz, CD_2Cl_2, 25 °C) δ: 7.30-7.56 (m, 8H, aryl-*H*), 7.01 (br s, 8H, B-C$_6$*H*$_5$), 7.01 (br s, 8H, B-C$_6$*H*$_5$), 6.86 (br s, 4H, B-C$_6$*H*$_5$), 5.20 (br s, 2H, central arene-*H*), 4.26-4.23 (m, 2H, central arene-*H*), 2.66-2.79 (m, 2H, C*H*(CH_3)$_2$), 2.54-2.67 (m, 2H, C*H*(CH_3)$_2$), 1.93 (s, 3H, NCC*H*$_3$), 1.19-1.37 (m, 12H, CH(C*H*$_3$)$_2$), 0.94-1.02 (m, 12H, CH(C*H*$_3$)$_2$), and -0.56 (t, 1H, *J* = 76.74 Mo-*H*). ^{13}C{^{1}H} NMR (101 MHz, CD_2Cl_2, 25 °C) δ: 163.69-165.16 (q, *J* = 49.90 Hz, B-*C*), 147.43 (d, *J* = 25.04

Hz, aryl-*C*), 141.01 (d, *J* = 29.00, aryl-*C*), 136.25 (s, B-C_6H_5), 131.25 (s, aryl-*C*H), 130.73 (s, aryl-*C*H), 128.54 (br d, *J* = 4.33 Hz, aryl-*C*H), 127.61 (d, *J* = 12.21, aryl-*C*H), 126.07 (s, B-C_6H_5), 124.93 (s, Mo-*C*NCH$_3$), 122.14 (s, B-C_6H_5), 106.54 (s, central arene-*C*), 80.32 (s, central arene-*C*H), 30.83 (d, *J* = 30.01 Hz, *C*H(CH$_3$)$_2$), 26.61 (d, *J* = 23.60, *C*H(CH$_3$)$_2$), 20.18 (s, CH(*C*H$_3$)$_2$), 19.35 (s, CH(*C*H$_3$)$_2$), 18.92 (s, CH(*C*H$_3$)$_2$), 18.20 (s, CH(*C*H$_3$)$_2$), and 4.65 (s, Mo-CN*C*H$_3$). $^{31}P\{^1H\}$ NMR (162 MHz, CD_2Cl_2, 25 °C) δ: 91.47. Anal. Calcd. for **7·DCM** $C_{57}H_{66}BCl_2MoNP_2$ (%): C, 68.14; H, 6.62; N, 1.39. Found: C, 68.57; H, 6.70; N, 1.93.

*Synthesis of **8***

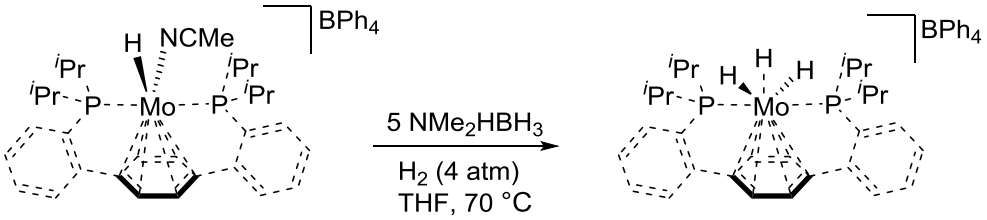

7 **8**

THF (5 mL) was added to a thick-walled Schlenk tube charged with **7** (102 mg, 0.110 mmol), Me_2NHBH_3 (53 mg, 0.832 mmol), and a stir bar. The solution was degassed by a single freeze-pump-thaw cycle. The orange homogeneous solution was frozen and the headspace was backfilled with *ca.* 4 atm of H_2 gas. Once at room temperature, the flask was placed in a 70 °C oil bath for 16 h with stirring. During this time, a color change to pale yellow was observed. Pentane (50 mL) was carefully added via cannula,[II] causing the precipitation of pale yellow solids. The solids were collected via vacuum filtration and washed with Et_2O (2 x 5 mL). The remaining solids were extracted with DCM (2 x 3 mL), giving a vibrant yellow filtrate. Volatiles were removed *in vacuo*, giving a mixture of yellow and white solids. Crystallization via pentane vapor diffusion into a concentrated THF solution removed the B-N reaction byproducts, providing pure **8** as X-ray quality crystalline yellow plates. ^1H NMR (300 MHz, CD_2Cl_2, 25 °C) δ: 7.37-7.59 (m, 8H, aryl-*H*), 7.32 (br s, 8H, B-aryl-*H*), 7.01 (br t, 8 H, *J* = 6.50, B-aryl-*H*), 6.68 (br t, 4H, *J* = 6.60, B-aryl-*H*), 5.56 (s, 4H, central arene-*H*), 2.43-2.54 (m, 4H, C*H*(CH$_3$)$_2$), 1.24-1.31 (m, 12H, CH(C*H*$_3$)$_2$), 0.97-1.03 (m, 12H, CH(C*H*$_3$)$_2$), and -4.64 (t, 3H, *J* = 29.72 Mo-*H*). $^{13}C\{^1H\}$ NMR (101 MHz, CD_2Cl_2, 25 °C) δ: 165.13-166.61 (q, *J* = 49.44 Hz, B-*C*), 143.89 (br d, *J* = 4.19 Hz, aryl-C), 143.65 (d, *J* = 15.99 Hz, aryl-*C*), 137.82 (s, B-C_6H_5), 133.34 (s, aryl-*C*H), 132.33 (br s, central arene-*C*), 131.84 (s, aryl-*C*H), 131.70 (br s, aryl-*C*H), 127.96-128.08 (m, aryl-C*H*), 127.51 (s, B-C_6H_5), 123.63 (s, B-C_6H_5), 91.16 (s, central arene-*C*H), 31.97 (d, *J* = 32.95, *C*H(CH$_3$)$_2$), 20.90 (s, CH(*C*H$_3$)$_2$), and 20.53 (s, CH(*C*H$_3$)$_2$). $^{31}P\{^1H\}$ NMR (121 MHz, CD_2Cl_2, 25 °C) δ: 97.70.

*Reaction of **8** with D_2*

A mixture of the isotopologs can be prepared via addition of 7 equiv. of D_2 (as measured by calibrated gas bulb) to a degassed CD_2Cl_2 solution of **8**. Unlike the dihydride **6**, the isotopologs of **8** are not resolved in the $^{31}P\{^1H\}$ NMR and as such, their relative ratio is unknown. Integration of the hydridic resonances is omitted. ^1H NMR (400 MHz, CD_2Cl_2, 25 °C) δ: 7.39-7.59 (m, 8H, aryl-*H*), 7.31 (br s, 8H, B-aryl-*H*), 7.00 (br t, 8 H, *J* = 6.50, B-aryl-*H*), 6.86 (br t, 4H, *J* = 6.82, B-aryl-*H*), 5.56 (s, 4H, central arene-*H*), 2.43-2.54 (m, 4H, C*H*(CH$_3$)$_2$), 1.26-1.30 (m, 12H, CH(C*H*$_3$)$_2$), 0.99-1.02 (m, 12H, CH(C*H*$_3$)$_2$), and -4.76 to -4.57 (tm, J_{HP} = 34.77, Mo-*H*). $^{31}P\{^1H\}$ NMR (162 MHz, CD_2Cl_2, 25 °C) δ: 96.64-96.80 (m).

Reactivity with AB Analogs

In a typical reaction, the Mo complex under investigation (**4-8**, 0.025 mmol) and the AB analog (NH_3BEt_3 or NMe_3BH_3, 0.125 mmol) were dissolved in THF. The resulting solution was transferred to a quartz J.

[II] CAUTION: Pressure builds up over the course of the reaction.

Young NMR tube. In the case of precatalyst **4**, NaBPh4 (17 mg, 0.050 mmol) was also added to the reaction mixture to aid in solubilizing the dication. The reactions were heated to 70 °C and monitored via ^{31}P NMR spectroscopy.

Time Resolved AB Dehydrogenation Experiments

In a typical reaction, a solution of catalyst (**4** or **8**, 0.010 mmol) and AB (2.3 mg, 0.075 mmol) in diglyme (0.500 mL) was transferred to quartz J. Young NMR tube. NaBPh4 (6.8 mg, 0.020 mmol) was added in reactions with **4** to aid in solubilizing the dication as well as acting as an internal standard for ^{11}B NMR experiments. The reactions were placed in a Varian 400 MHz NMR spectrometer preheated to 70 °C. Successive ^{11}B and ^{31}P{^{1}H} NMR spectra were recorded. See figures S23-S24.

NH_2BH_2 Trapping Experiments

In a typical reaction, a quartz J. Young NMR tube was charged with precatalyst (**4** or **5**, 0.020 mmol), AB (1.2 mg, 0.040 mmol), and diglyme (0.5 mL). Cyclohexene (61 µL, 0.600 mmol) was added via microsyringe and the tube was sealed and placed in a Varian 400 MHz NMR spectrometer preheated to 70 °C. Successive ^{11}B and ^{31}P{^{1}H} NMR spectra were recorded. See figures S25-S26.

Eudiometric Measurement Details

In a typical run, a 2 mL Schlenk tube was charged with precatalyst (0.0125 mmol), AB (7.7 mg, 0.250 mmol), diglyme (1 mL) and a stir bar. The Schlenk tube was sealed and attached to the eudiometer depicted in Figure S1. The tubing attached to the Schlenk tube was evacuated and backfilled with N_2 (x3). Under positive N_2 pressure, the flask was opened to the burette, causing immediate bubbling. Once the pressure had equilibrated, the Schlenk tube was quickly opened and closed to alleviate positive pressure remaining from the drybox. Once bubbling stopped, the initial volume was recorded. The Schlenk tube was submerged in a 70 °C oil bath, with stirring, and opened. Gas evolution was monitored over time.

Precatalysts **5**, **9**, and **11**, formed homogeneous solutions under the above described conditions. Complex **4** proved only slightly soluble in diglyme, but rapidly formed a homogeneous red/orange solution upon heating the in the presence of AB. In case of **4**, **5**, and **11**, homogeneity was maintained until the majority of the H_2 had been liberated, at which point the forming solids were assumed to be dehydrogenation byproducts (namely PB). Experiments utilizing complex **9** remained homogeneous throughout the 6.5 h experiment. Diglyme solutions of complex **10** appeared to remain homogeneous, but at the employed concentrations, the deep green solution proved too darkly colored to be certain.

For catalyst reusability reactions, following a run set up as described above, the 3-way valve was used to place the reaction vessel under positive N_2 pressure. The Teflon tap was removed and additional dry AB was added with a backflow of N_2. The Schlenk tube was sealed, the pressure in the eudiometer allowed to equalize, and H_2 evolution measurement resumed.

Catalyst reuse was first explored using conditions analogous to those employed for single-use dehydrogenation measurements. In a typical run, a 2 mL Schlenk tube was charged with precatalyst (0.017 mmol), AB (10.5 mg, 1.62 mmol), diglyme (1.00 mL) and a stir bar. The Schlenk tube was sealed and attached to the eudiometer as described above. The Schlenk tube was submerged in a 70 °C oil bath, with stirring, and opened. Gas evolution was monitored over time. Every 4 h (for complex **4**) or 6 h (for complex **5**), an additional charge of AB (10.5 mg, 1.62 mmol) was added with N_2 counter pressure. Turnover number was calculated from the moles of H_2 produced and system weight percent hydrogen was determined according to the following formula:[11]

$$\left(\frac{Theor.Wt.Yield\ H_2}{Wt.AB + Wt.Diglyme + Wt.Precatalyst}\right) * \left(\frac{Tot.H_2\ Collected}{Theor.H_2\ Content}\right) * 100\% = System\ Wt.\%\ H_2$$

In an attempt to increase the system weight percent, conditions similar to those reported by Williams and coworkers were used.[11] In a typical reaction, a 2 mL Schlenk tube was charged with precatalyst (0.0017 mmol), AB (50.0 mg, 1.62 mmol), diglyme (0.100 mL) and a stir bar, providing a slurry comprised of *ca.* 16 M AB. The Schlenk tube was sealed and attached to the eudiometer as described above. The Schlenk tube was submerged in a 70 °C oil bath, with stirring, and opened. Gas evolution was monitored over time. Every 6 h, an additional charge of 50 mg of AB and 0.100 mL of diglyme was added with N_2 counter pressure. Turnover number and system weight percent hydrogen were calculated as before.

The effect of H_2O and methanol on dehydrogenation catalysis was determined as follows. In a typical reaction, a 2 mL Schlenk tube was charged with precatalyst (0.017 mmol), AB (10.5 mg, 1.62 mmol), diglyme (1.00 mL) and a stir bar. The Schlenk tube was sealed and attached to the eudiometer as described above. With a backflow on N_2, the Teflon pin was removed and replaced with a rubber septum. Degassed H_2O or MeOH (2 μL) was added via microsyringe. The septum was removed and the Teflon pin replaced. The 3-way valve was turned to connect the reaction vessel and the upturned burette and following pressure equilibration, the Schlenk tube was submerged in a 70 °C oil bath, with stirring, and opened. Gas evolution was monitored over time. Alternatively, unpurified (benchtop) AB was used in lieu of sublimed AB in the absence of added water as described above.

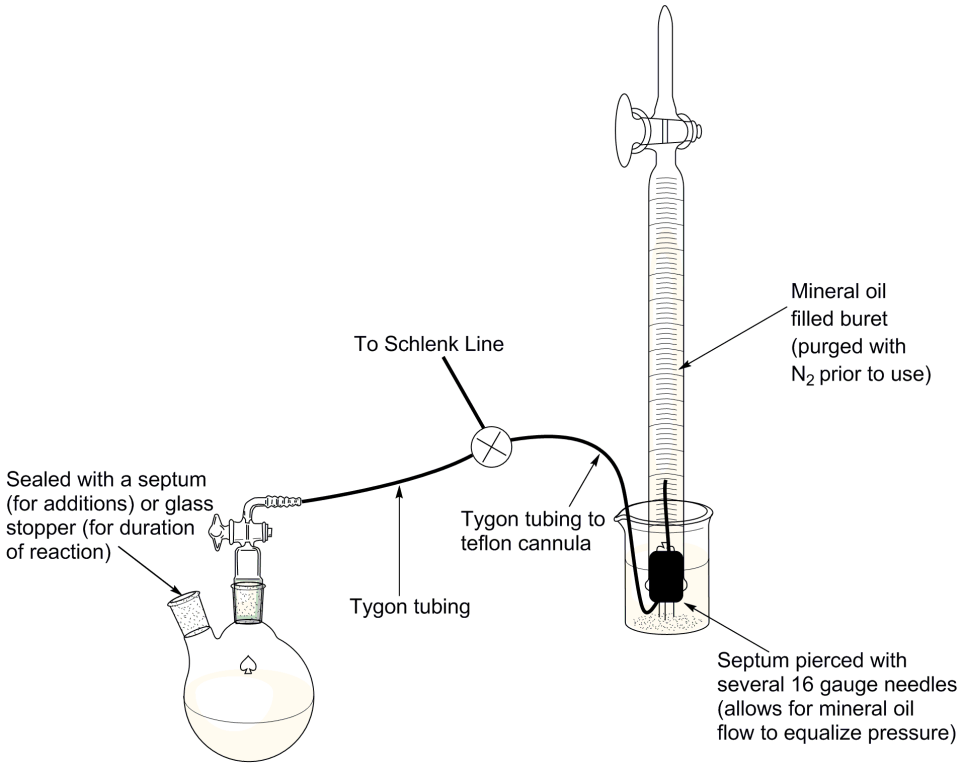

Figure S1. Schematic for the eudiometer apparatus used for ammonia borane dehydrogenation reactions. Note that rather than a 2-neck round bottom flask as depicted above, a Teflon valve Schlenk tube was used for all reported reactions.

Reaction Kinetics Measurements

In a typical reaction, a quartz J. Young NMR tube was charged with precatalyst (**4** or **5**, 0.009 mmol), AB (5.6 mg, 0.180 mmol), $NaBPh_4$ (30.8 mg, 0.09 mmol) and diglyme (0.5 mL). Tube was sealed[III] and placed in a Varian 400 MHz NMR spectrometer preheated to 70 °C. ^{11}B NMR spectra were recorded as an array utilizing the pre-acquisition delay mechanism in Agilent's VnmrJ software. Relative AB concentration was determined via integration of the AB resonance with respect to $NaBPH_4$.

[III] CAUTION: Pressure builds up over the course of the reaction.

NMR Spectra

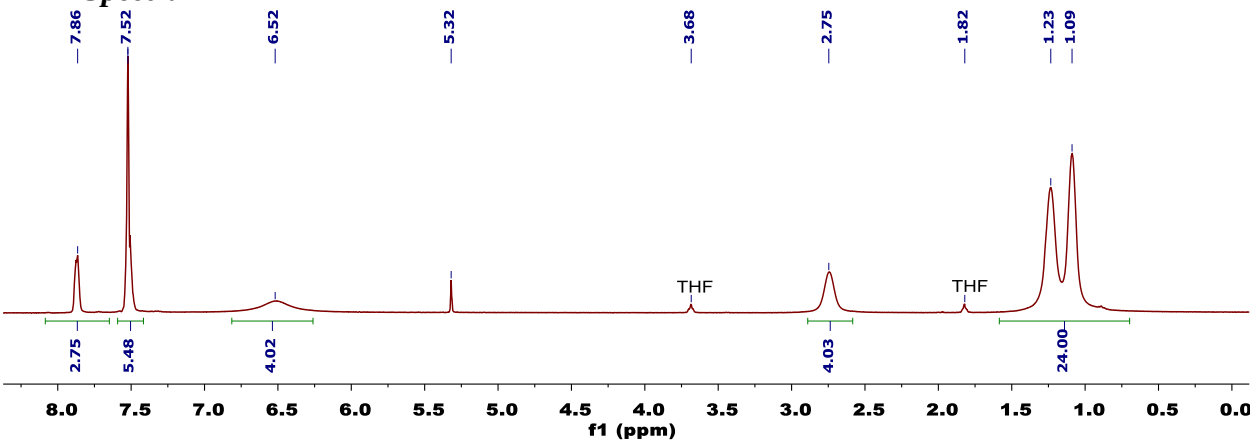

Figure S2—^{1}H NMR Spectrum (500 MHz, CD_2Cl_2) of **2**.

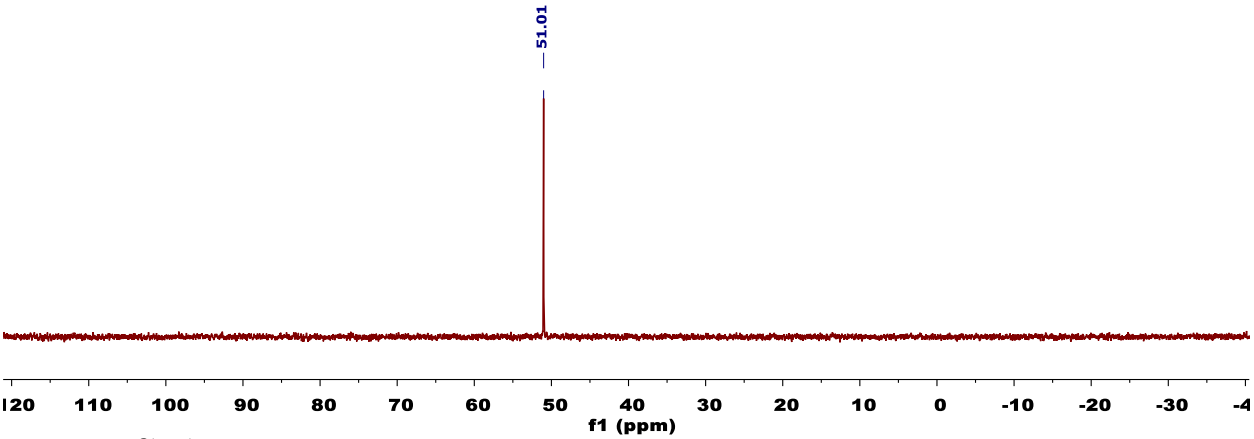

Figure S3—^{31}P{^{1}H} NMR Spectrum (121 MHz, CD_2Cl_2) of **2**.

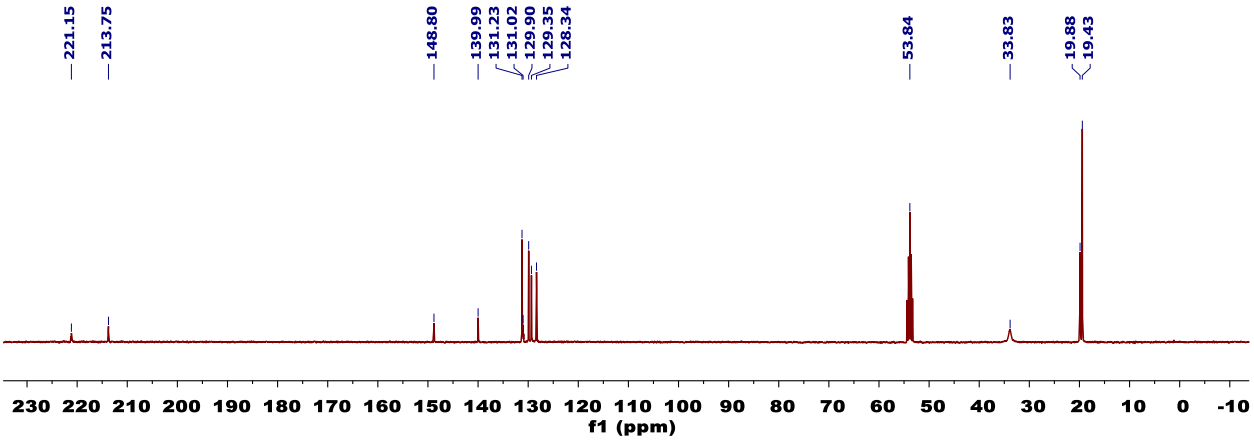

Figure S4—^{13}C{^{1}H} NMR Spectrum (101 MHz, CD_2Cl_2) of **2**.

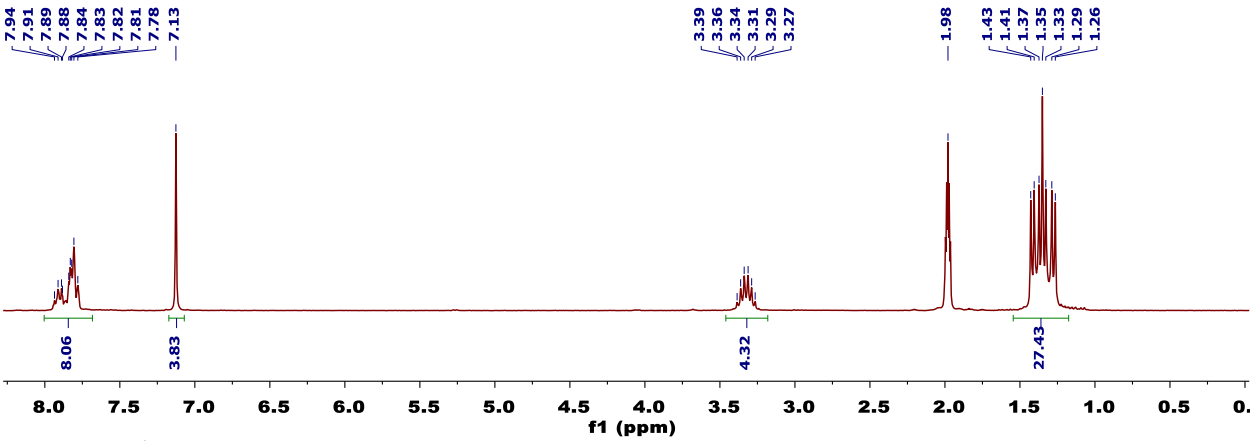

Figure S5—^{1}H NMR Spectrum (300 MHz, CD_3CN) of **3**.

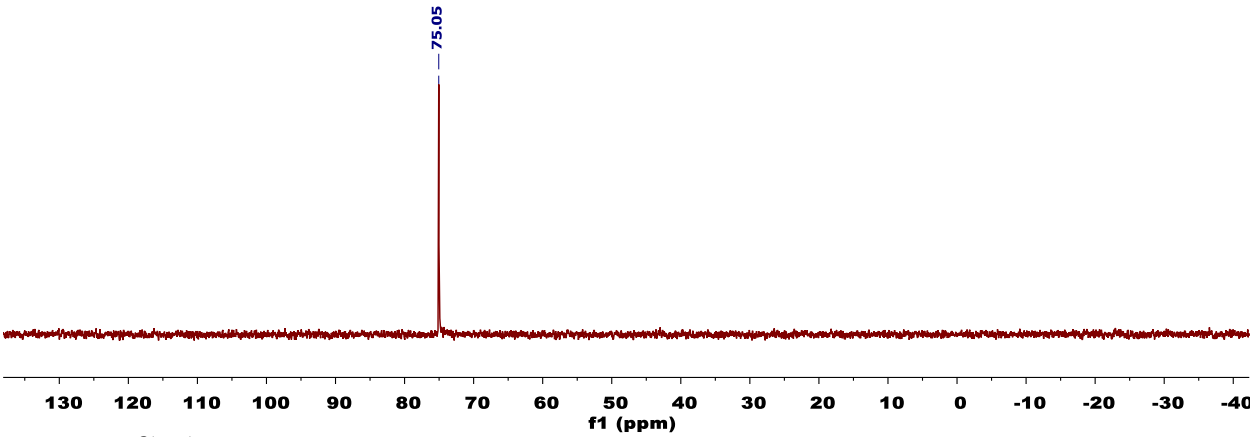

Figure S6—$^{31}P\{^{1}H\}$ NMR Spectrum (121 MHz, CD_3CN) of **3**.

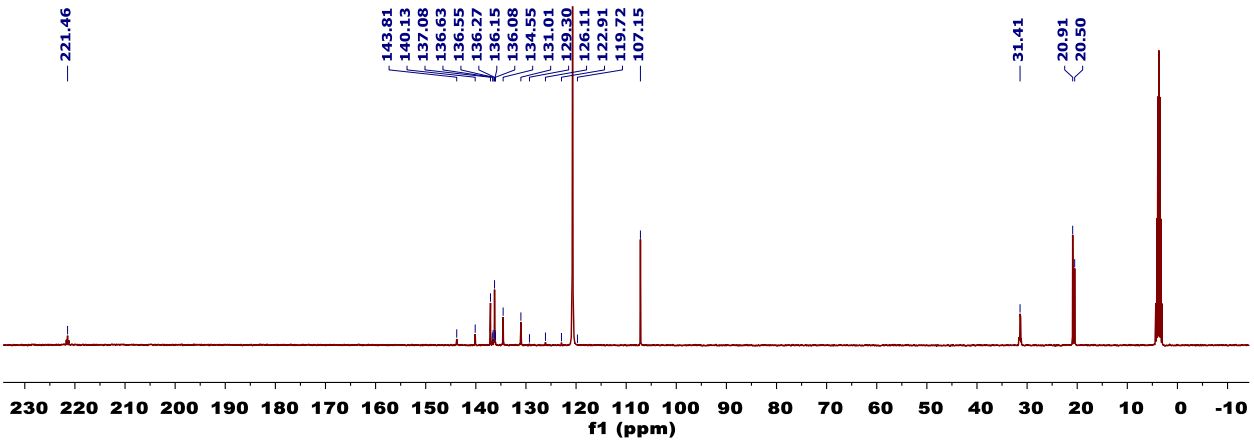

Figure S7—$^{13}C\{^{1}H\}$ NMR Spectrum (101 MHz, CD_3CN) of **3**.

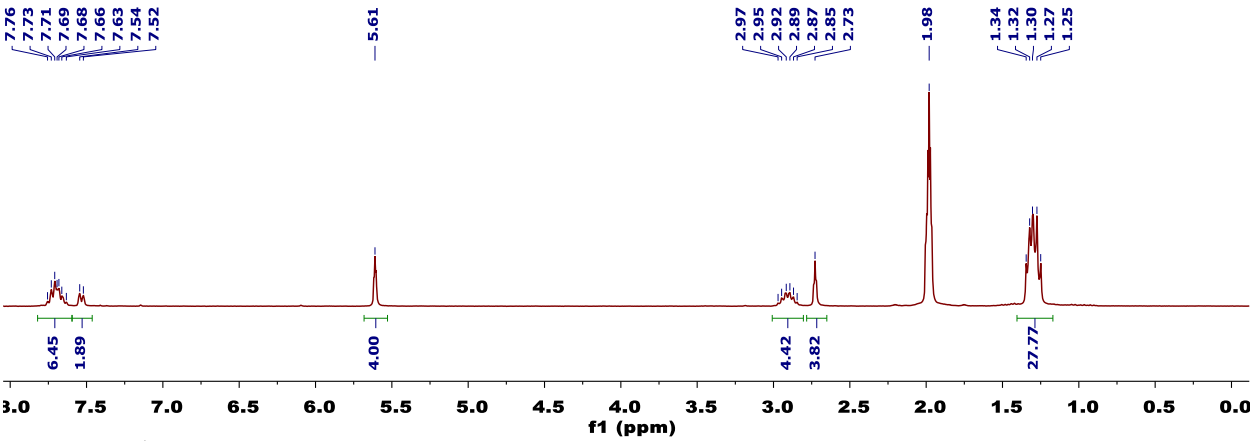

Figure S8—^{1}H NMR Spectrum (300 MHz, CD_3CN) of **4**.

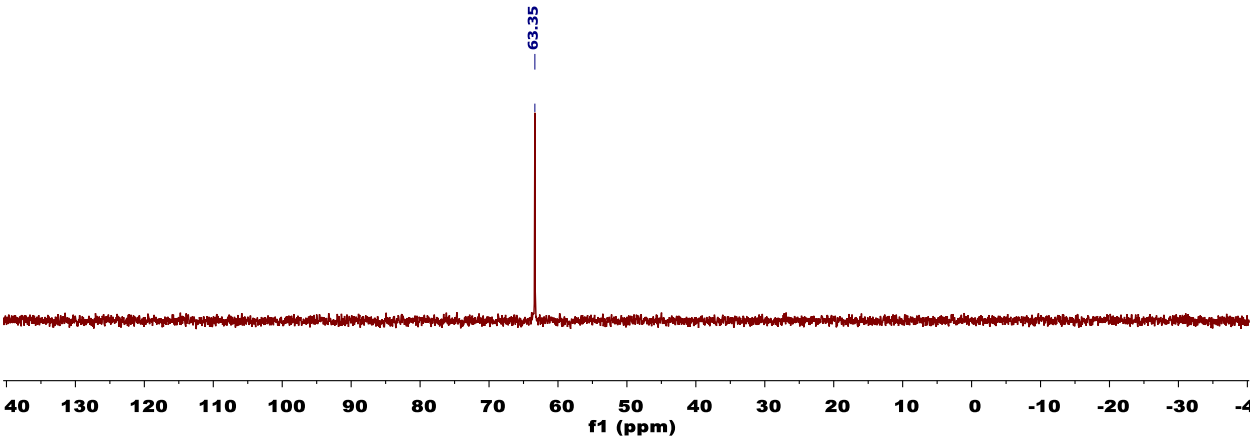

Figure S9—$^{31}P\{^{1}H\}$ NMR Spectrum (121 MHz, CD_3CN) of **4**.

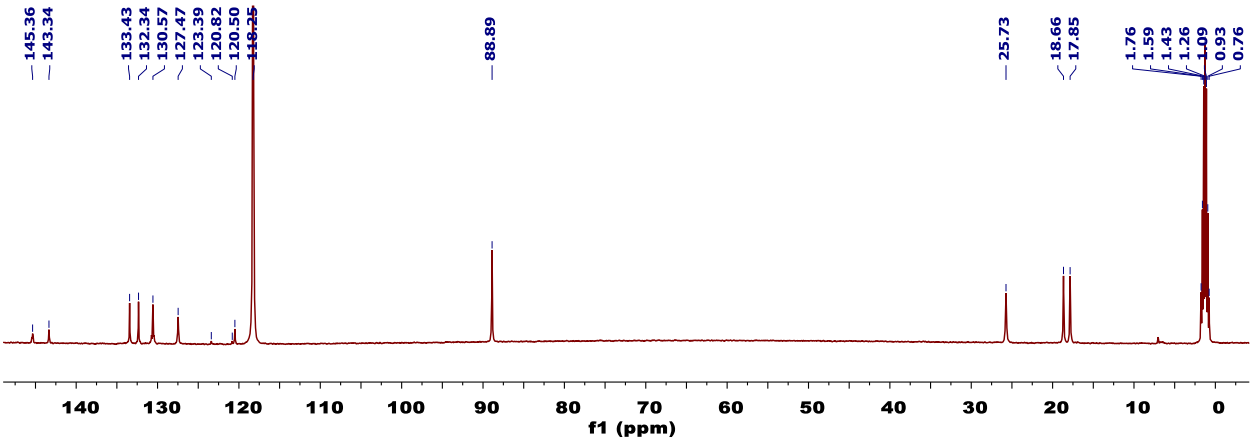

Figure S10—$^{13}C\{^{1}H\}$ NMR Spectrum (126 MHz, CD_3CN) of **4**.

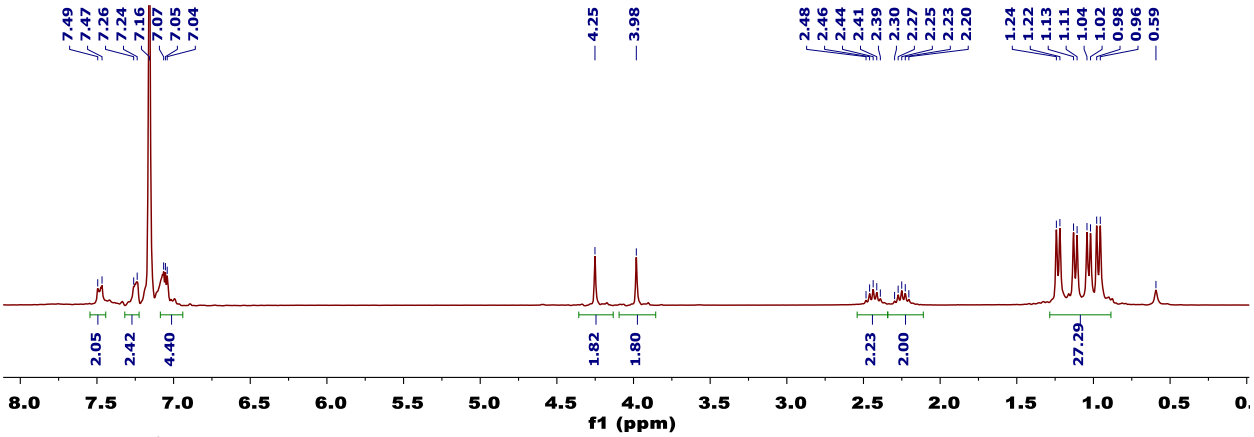

Figure S11—^{1}H NMR Spectrum (300 MHz, C_6D_6) of **5**.

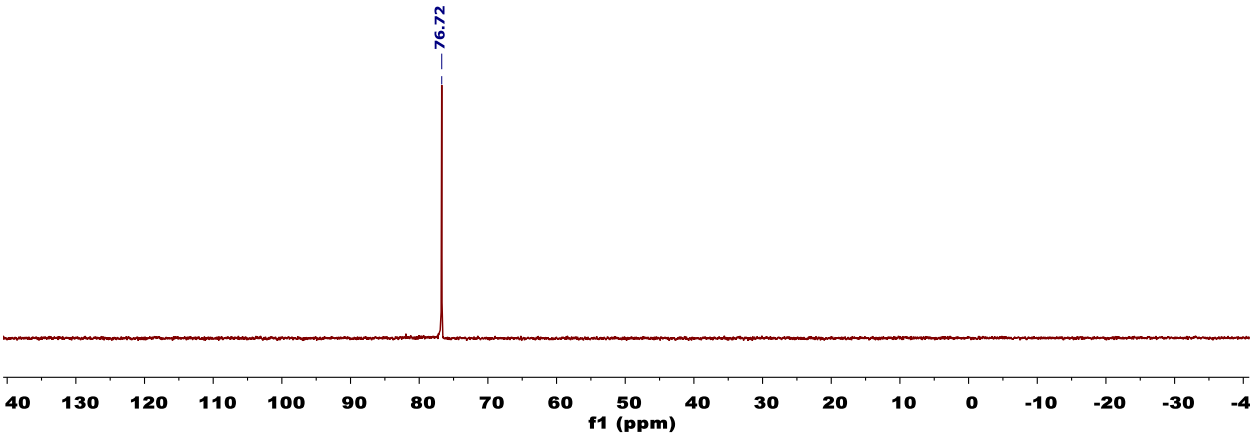

Figure S12—^{31}P{^{1}H} NMR Spectrum (121 MHz, CD_2Cl_2) of **5**.

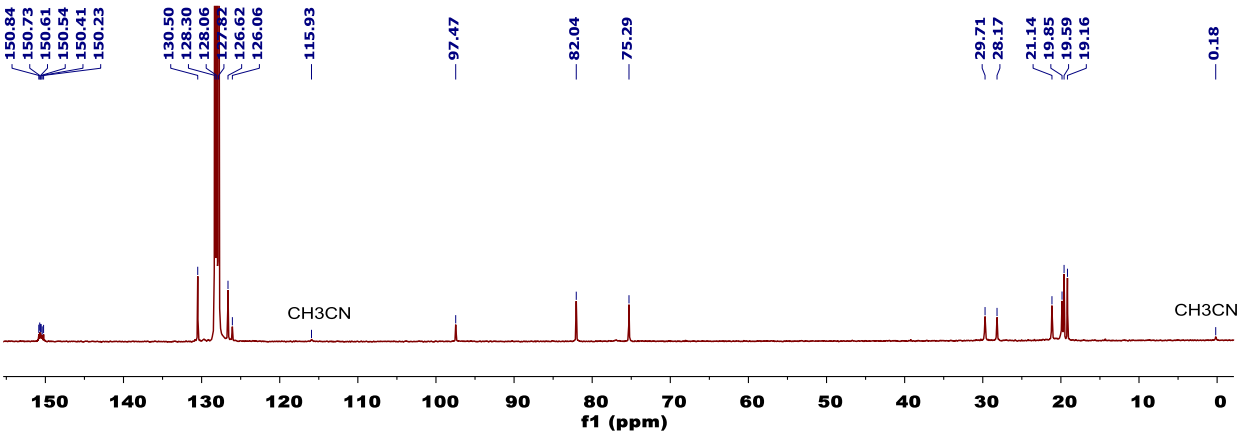

Figure S13—^{13}C{^{1}H} NMR Spectrum (101 MHz, C_6D_6) of **5**.

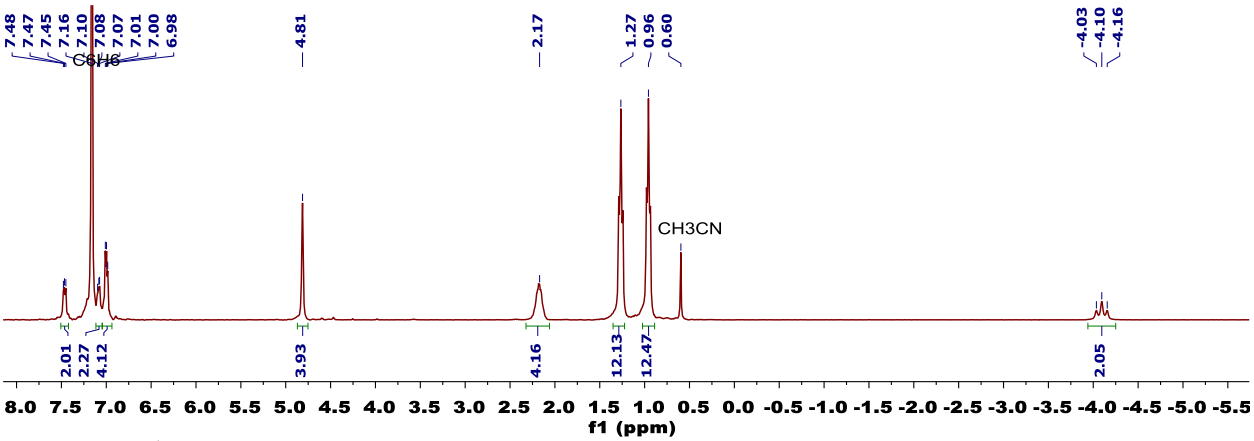

Figure S14—^{1}H NMR Spectrum (300 MHz, C_6D_6) of **6**.

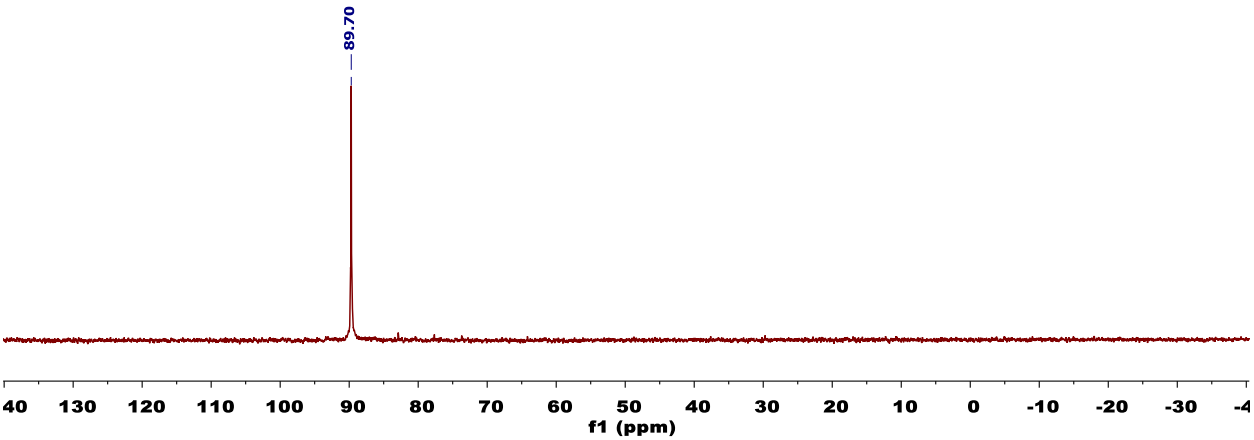

Figure S15—^{31}P{^{1}H} NMR Spectrum (121 MHz, C_6D_6) of **6**.

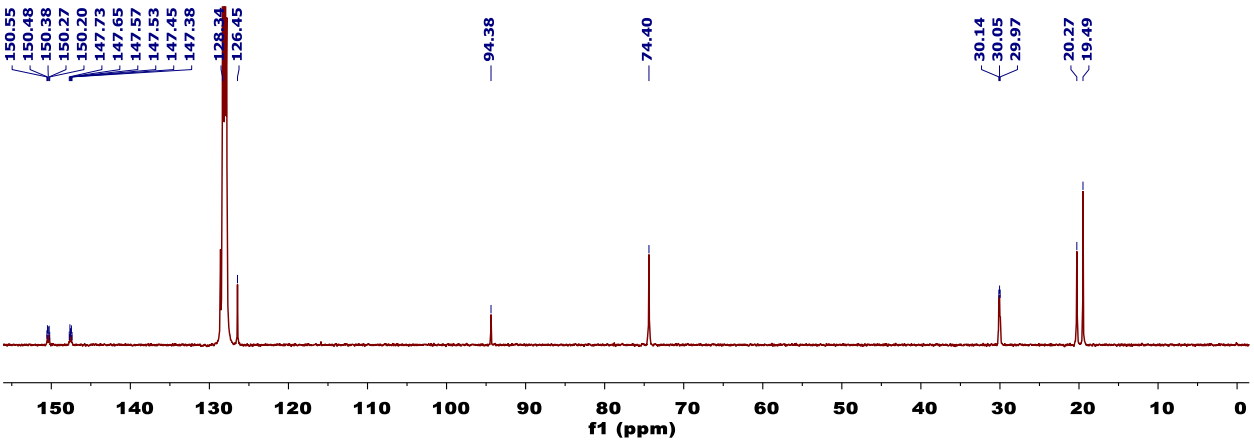

Figure S16—^{13}C{^{1}H} NMR Spectrum (126 MHz, C_7D_8) of **6**.

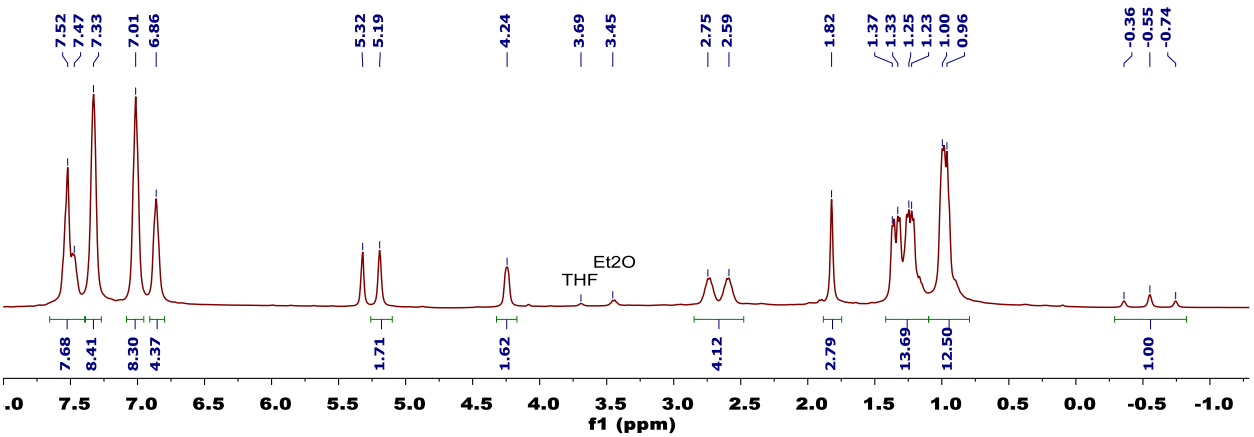

Figure S17—^{1}H NMR Spectrum (400 MHz, CD_2Cl_2) of **7**.

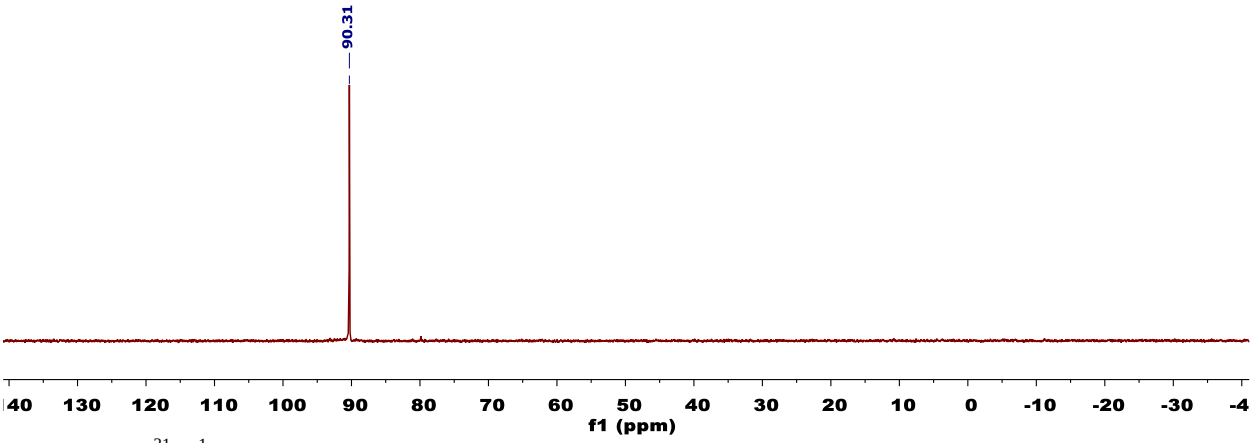

Figure S18—$^{31}P\{^{1}H\}$ NMR Spectrum (162 MHz, CD_2Cl_2) of **7**.

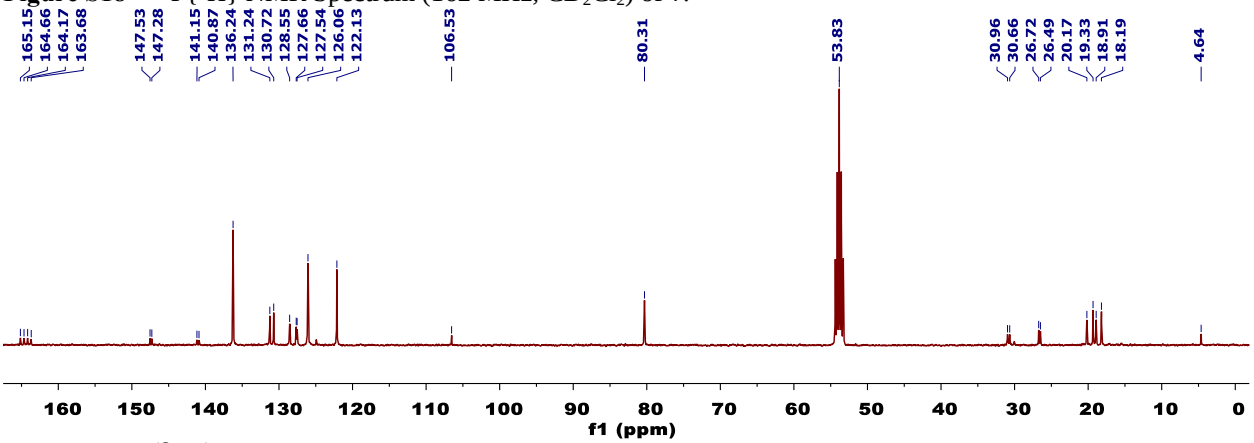

Figure S19—$^{13}C\{^{1}H\}$ NMR Spectrum (101 MHz, CD_2Cl_2) of **7**.

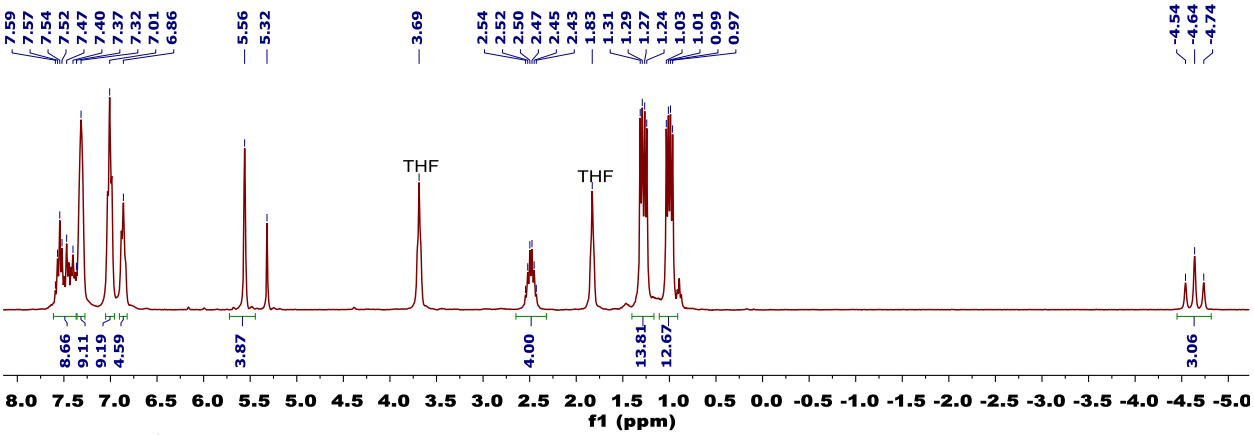

Figure S20—^{1}H NMR Spectrum (300 MHz, CD_2Cl_2) of **8**.

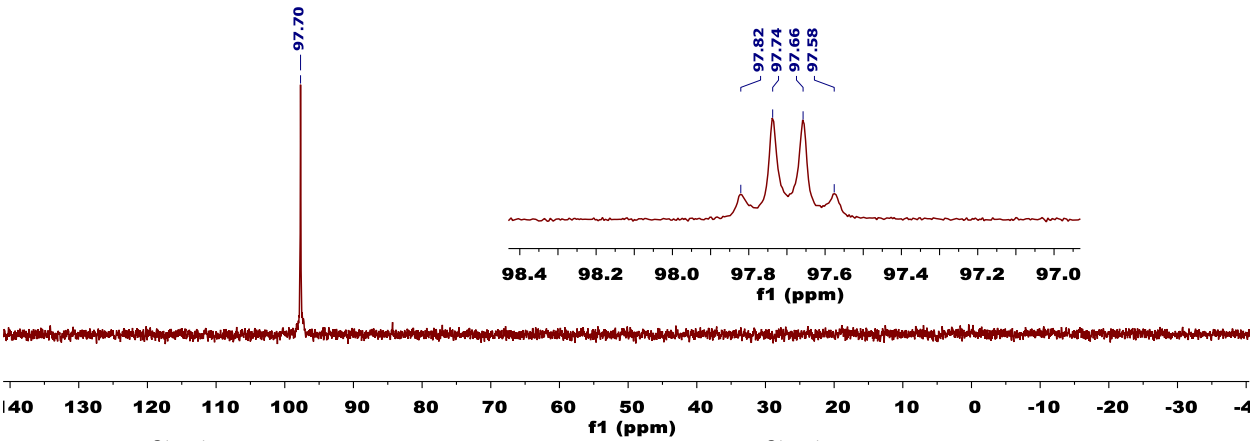

Figure S21—^{31}P{^{1}H} NMR Spectrum (121 MHz, CD_2Cl_2) of **8**. Inset: ^{31}P{^{1}H} NMR Spectrum (162 MHz, CD_2Cl_2) of **8** with the proton decoupler centered at 7.0 ppm (selective hydride coupling).

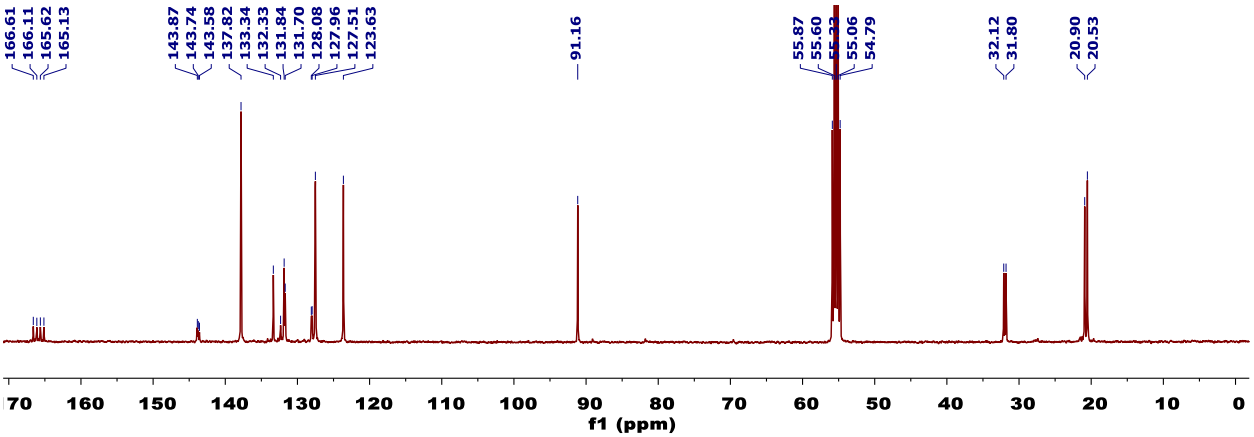

Figure S22—^{13}C{^{1}H} NMR Spectrum (101 MHz, CD_2Cl_2) of **8**.

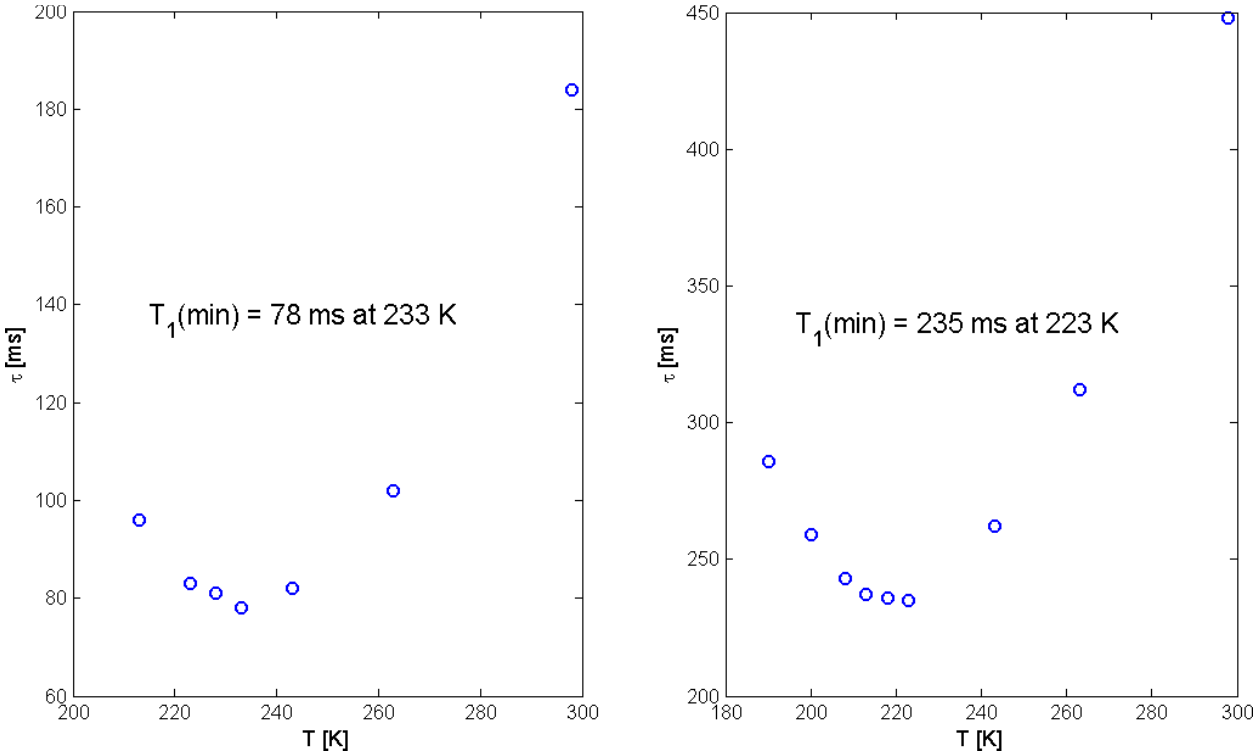

Figure S23—Plots of T_1 vs. T for **6** (left) and **8** (right).

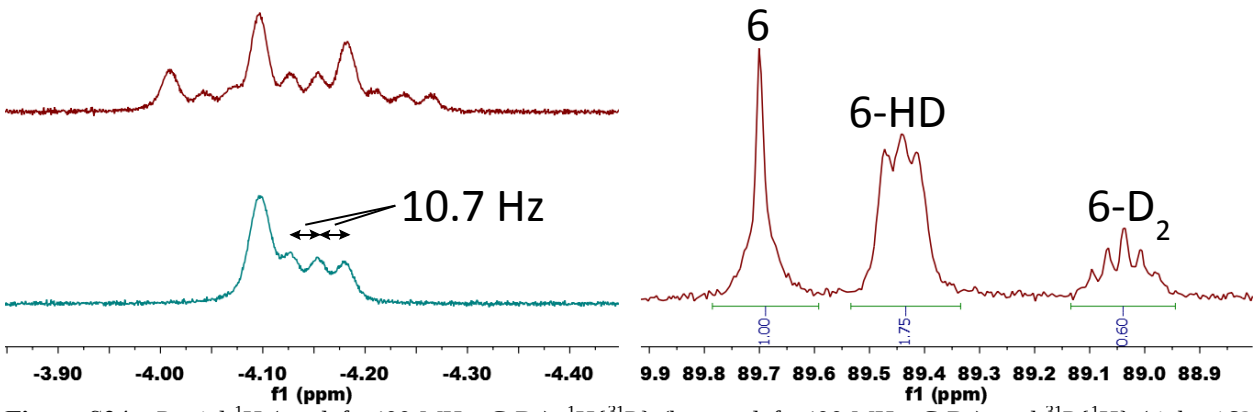

Figure S24—Partial ^1H (top left, 400 MHz, C_6D_6), $^1H\{^{31}P\}$ (bottom left, 400 MHz, C_6D_6), and $^{31}P\{^1H\}$ (right, 162 MHz, C_6D_6) NMR spectra of a mixture of **6**, **6-HD**, and **6-D$_2$**. The observed J_{HD} of 10.7 Hz is consistent with a contracted Mo dihydride complex.[12]

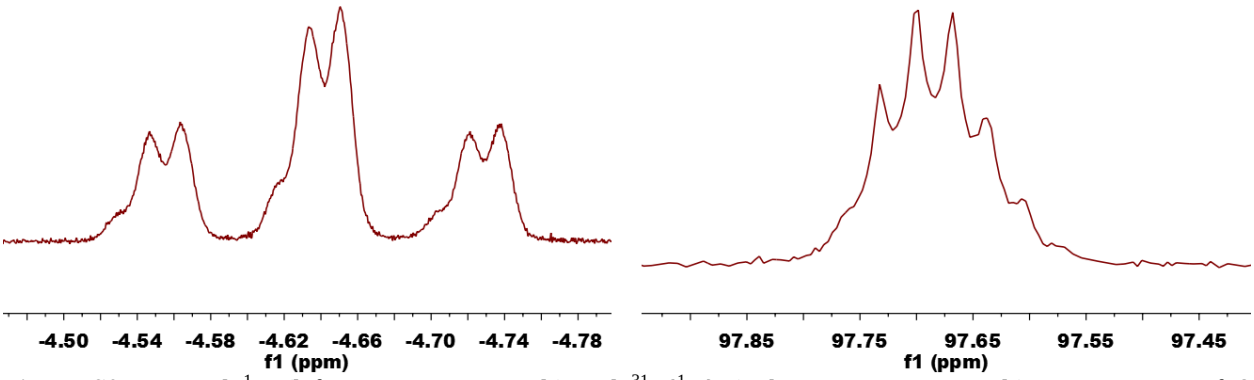

Figure S25—Partial ^{1}H (left, 400 MHz, CD_2Cl_2) and $^{31}P\{^{1}H\}$ (right, 162 MHz, CD_2Cl_2) NMR spectra of **8** following treatment with ca. 7 equiv. of D_2. Unresolved isotopologue resonances have been reported for other classical Mo trihydride complexes.[13]

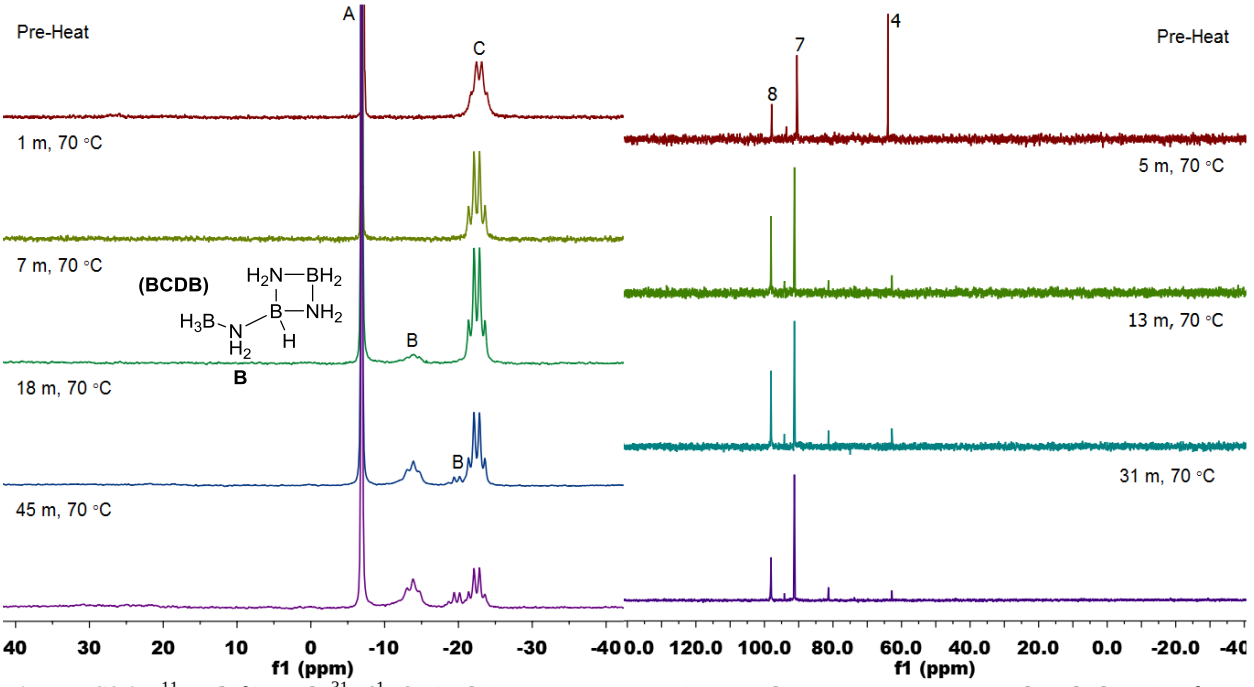

Figure S26—^{11}B (left) and $^{31}P\{^{1}H\}$ (right) NMR spectra (128 and 162 MHz respectively, diglyme) of AB dehydrogenation by **4**. In the ^{11}B NMR spectra, the internal $NaBPH_4$ standard (*A*) and AB (*C*) were initially observed. Over 45 mins, AB was consumed with concomitant generation of BCDB (*B*, inset). The $^{31}P\{^{1}H\}$ NMR spectrum shows formation of **8** and **7** from **4**, even prior to heating.

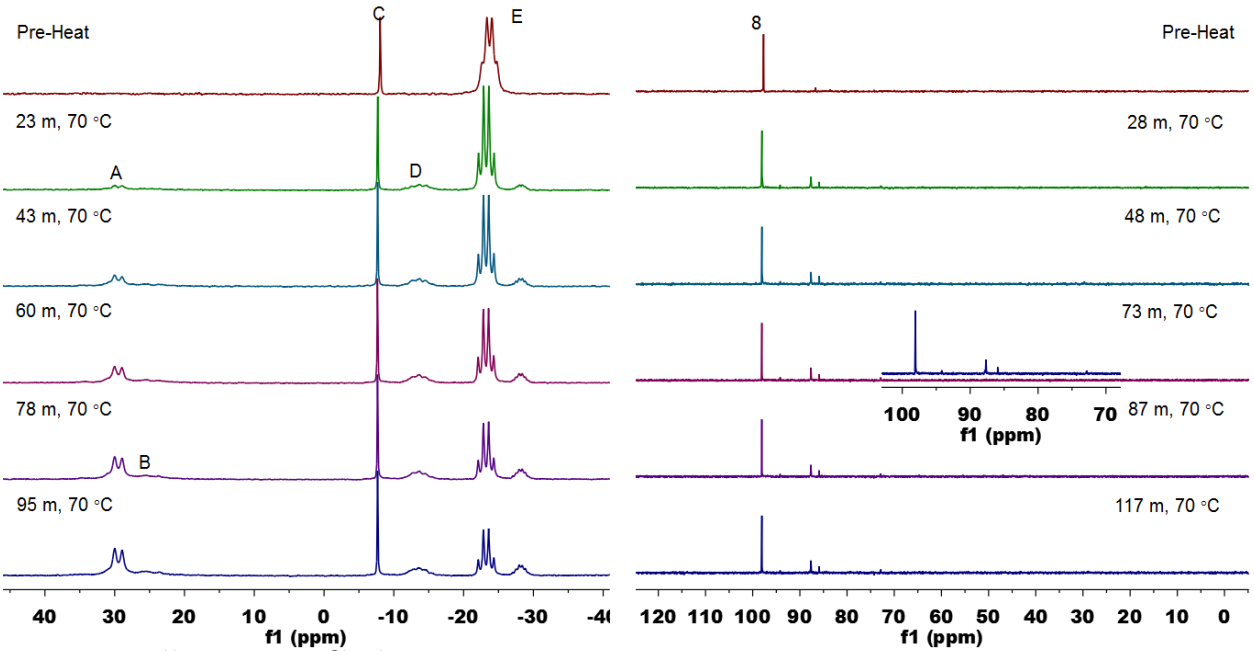

Figure S27—^{11}B (left) and ^{31}P{^{1}H} (right) NMR spectra (128 and 162 MHz respectively, diglyme) of AB dehydrogenation by **8.** In the ^{11}B NMR spectra, borazine (*A*) and PB (*B*) grow in with time. The formation of BCBD (*D*) is observed with the concomitant consumption of AB (*E*). A resonance for the BPh_4^- counterion of **8** is also observed. The ^{31}P{^{1}H} NMR spectrum shows formation of several species (see inset), with the most prominent starting to form prior to heating.

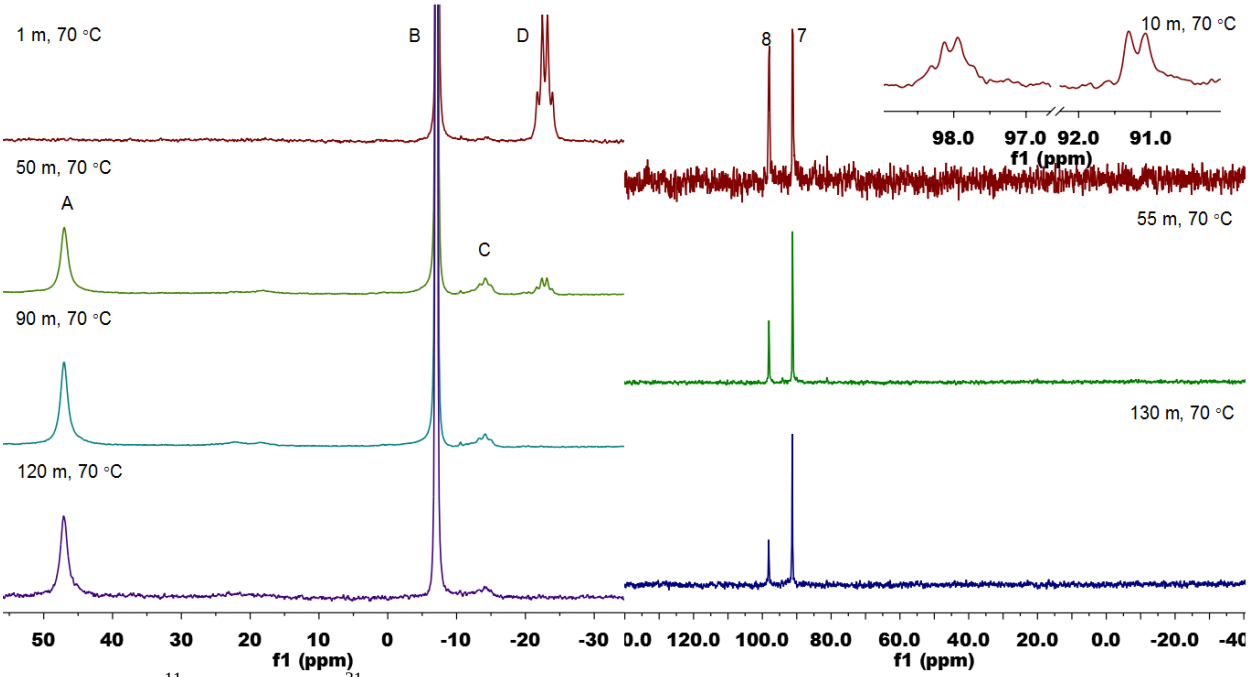

Figure S28—^{11}B (left) and ^{31}P (right) NMR spectra (128 and 162 MHz respectively, diglyme) of AB dehydrogenation by **4** in the presence of cyclohexene and the internal standard $NaBPh_4$ (*B*). The formation of the hydroborylation product $H_2NB(Cy)_2$ (*A*) is observed, along with consumption of AB (*D*). Some BCDB (*C*) was also generated. The selectively coupled ^{31}P NMR spectrum (top left) shows that **4** is consumed completely within 10 m, furnishing **7** (doublet) and **8** (quartet). Subsequent ^{31}P NMR spectra were proton decoupled to increase the signal to noise ratio.

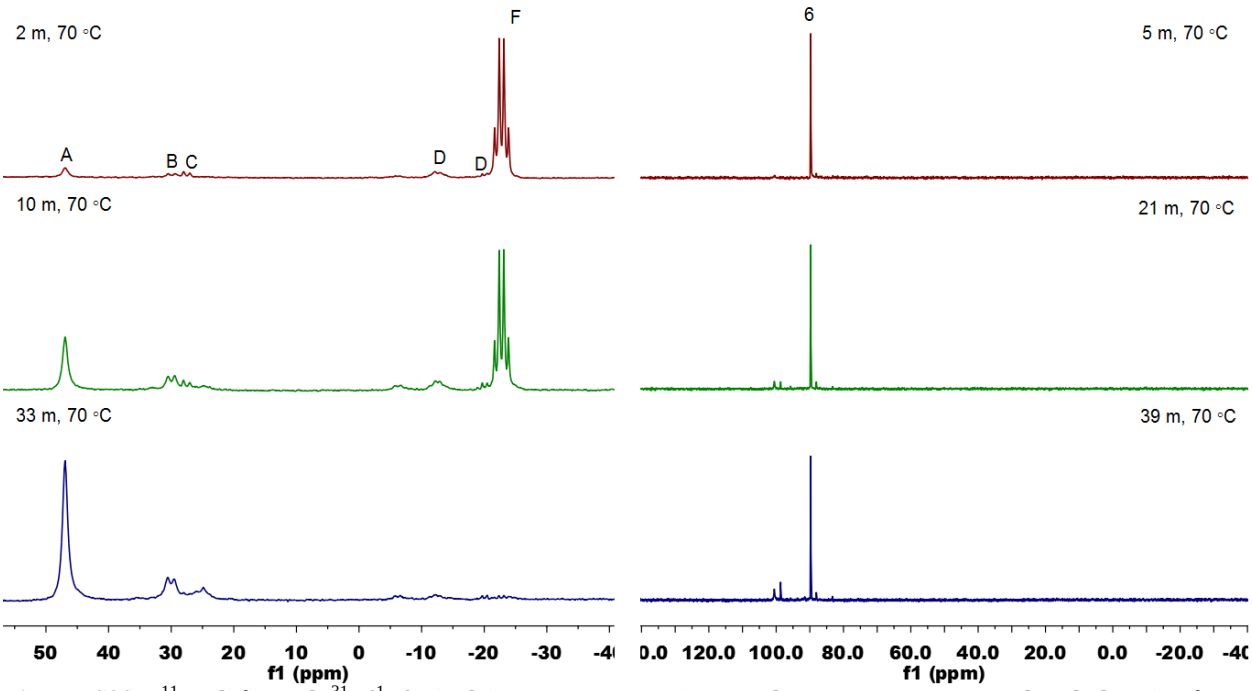

Figure S29—^{11}B (left) and $^{31}P\{^{1}H\}$ (right) NMR spectra (128 and 162 MHz respectively, diglyme) of AB dehydrogenation by **5** in the presence of cyclohexene. The formation of the hydroborylation product $H_2NB(Cy)_2$ (*A*) is observed, along with consumption of AB (*F*). Some BCDB (*D*), borazine (*B*), and PB (*C*) were also generated. The $^{31}P\{^{1}H\}$ NMR shows that **5** is consumed completely within 5 m, and **6** is the major species throughout the reaction.

Eudiometric Data

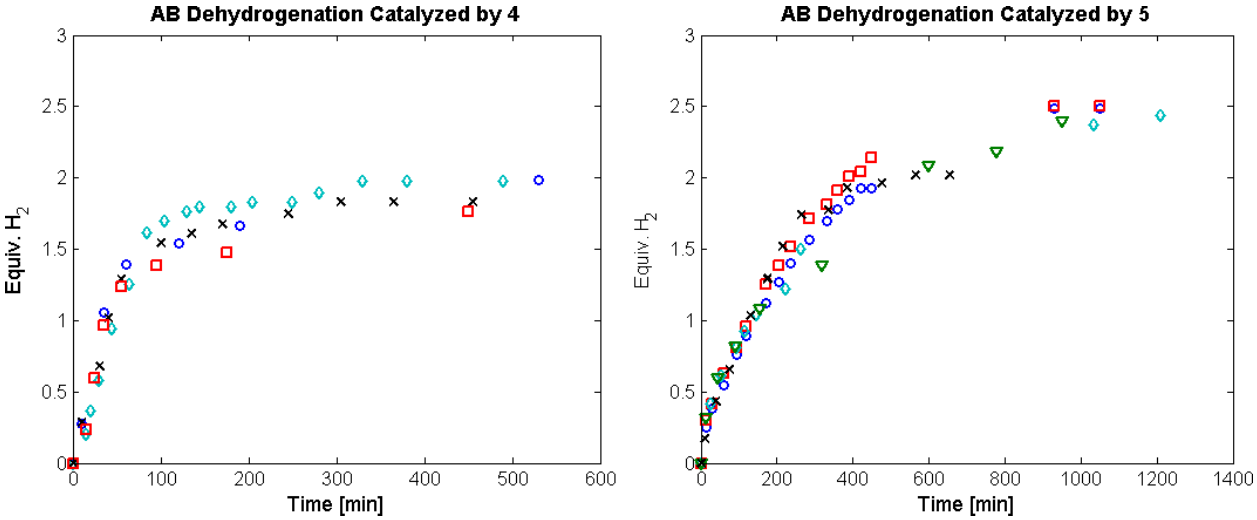

Figure S30—Hydrogen evolution measurements for **4** (left) and **5** (right). Addition of elemental mercury was observed to have no effect on the rate of catalysis (black x's). Mercury addition did lessen the extent of dehydrogenation catalysis from precatalyst **5**.

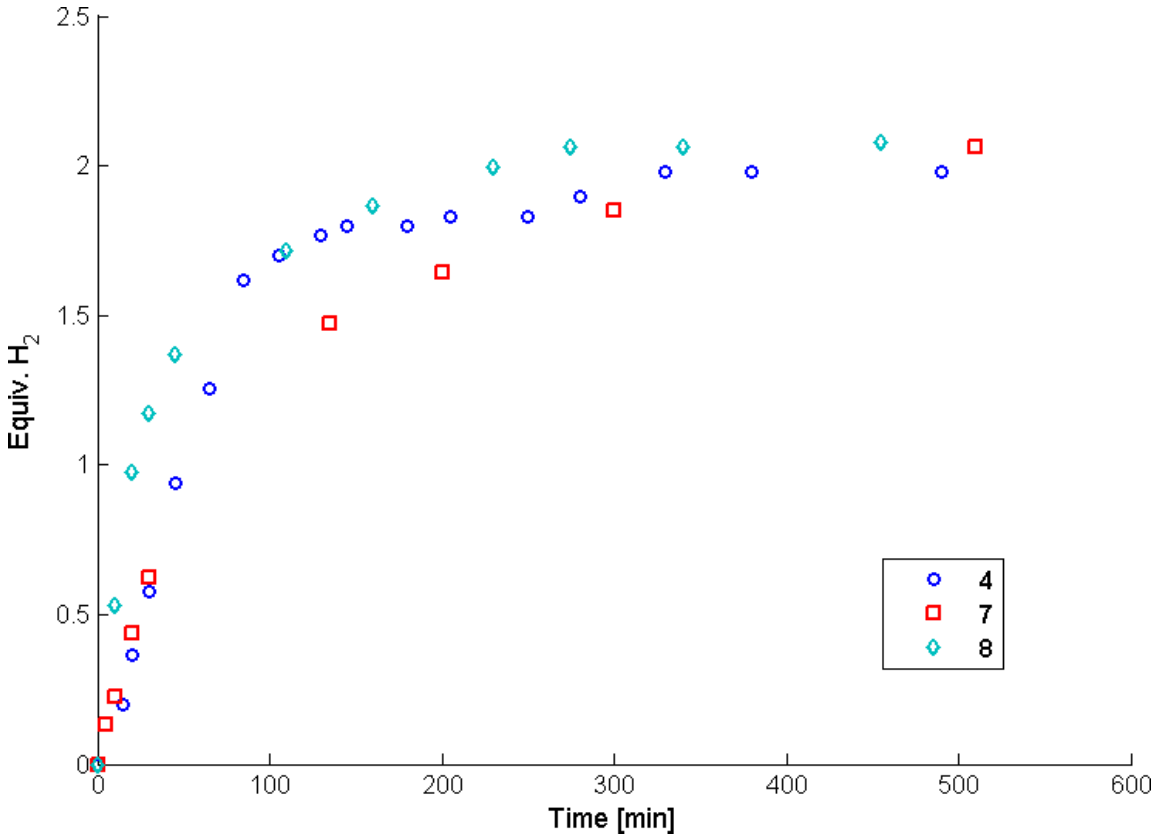

Figure S31—Eudiometric measurements displaying the kinetic competence of **4**, **7**, and **8**.

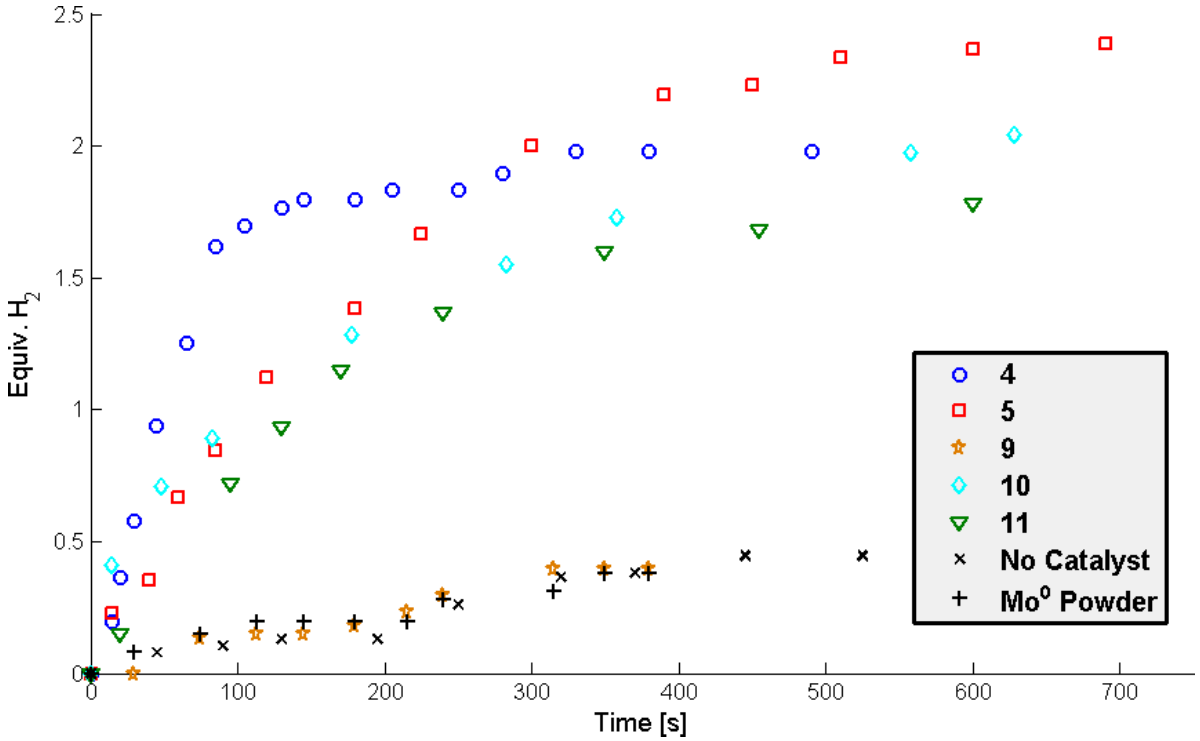

Figure S32—Hydrogen evolution profiles for Mo catalyzed AB dehydrogenation. Control reactions with AB in the absence of a catalyst and in the presence of Mo^0 powder are included for reference.

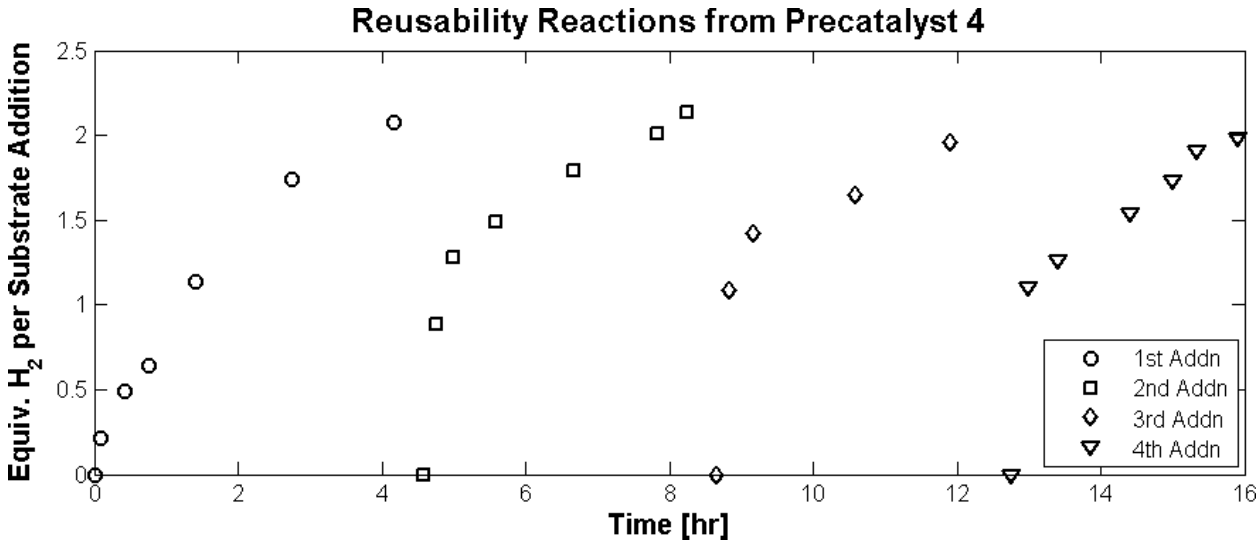

Figure S33—Multiple substrate additions to the reaction of AB with 5 mol % **4**. No decrease in the rate or extent of catalysis is observed over four squential *ca.* 4 hour experiments. A total of 2.0 equiv. of H_2 per AB molecule were released, indicating 274 turnovers. This corresponds to the liberation of 0.80 system wt. % H_2 (out of a possible 1.18 %).

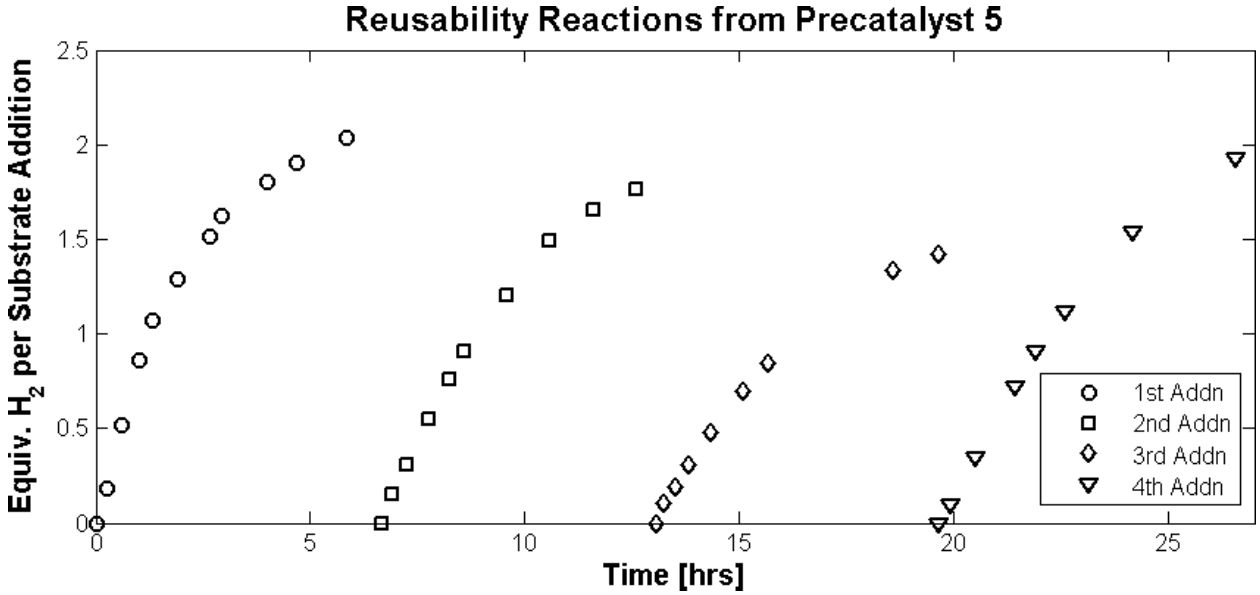

Figure S34—Multiple substrate additions to the reaction of AB with 5 mol % **5**. A slight decrease in the extent of catalysis is observed for the second and third addition. A total of 1.8 equiv. of H_2 per AB molecule were released, indicating 143 turnovers. This corresponds to the liberation of 0.52 system wt. % H_2 (out of a possible 0.88 %).

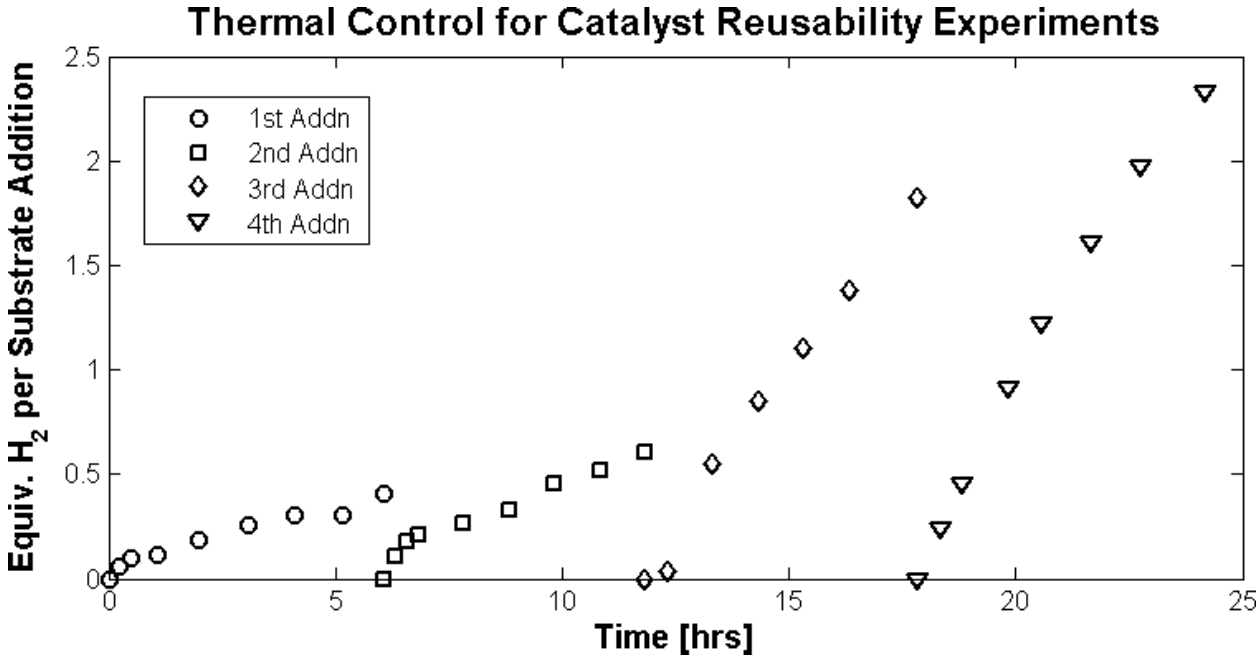

Figure S35—Multiple substrate additions to the thermal control reaction of heating *ca.* 0.25 M AB solutions in diglyme. No decrease in the rate or extent of catalysis is observed over four squential *ca.* 4 hour experiments. A total of 1.25 equiv. of H_2 per AB was collected, a significant decrease from the catalyzed systems (2.04 equiv. for **4** and 1.78 equiv. for **5**, respectively).

During the control, the marked difference in the rate of dehydrogenation observed between the first and latter two additions of AB is attributed to the second-order decomposition process for thermal dehydrogenation.[14] As the concentration of AB inceases with subsequent substrate additions, thermal dehydrogenation becomes more kinetically viable, leading to rapid H_2 release in the third and fourth runs.

The system weight percent H_2 released from the above systems is low in comparison to reported values;[11,15] however, this is largely a manifestation of the concentration of AB in solution. The majority (93 %) of the system weight can be attributed to the solvent. To attempt to increase system weight percent H_2, dehydrogenation was attempted at higher AB concentrations and lower catalyst loadings.

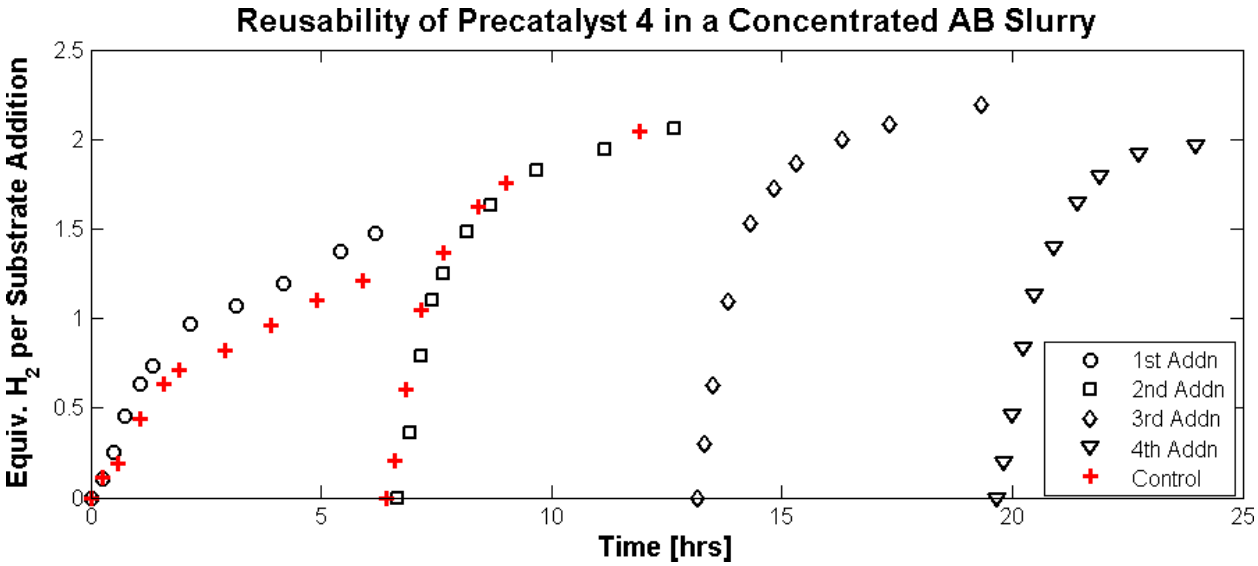

Figure S36—Multiple substrate additions to 0.1 mol % **4** in a *ca.* 16 M slurry of AB. The thermal control (identical conditions sans catalyst) is overlayed in red. Although a slight deviation between the catalyzed run and the control is observed for the first addition, no difference is observed following the second addition. Notably, this system achieves 4.4 wt. % H_2 release. The similarity of the catalyzed and control experiments eliminates the ability to attribute dehydrogenation activity to **4** under these conditions.

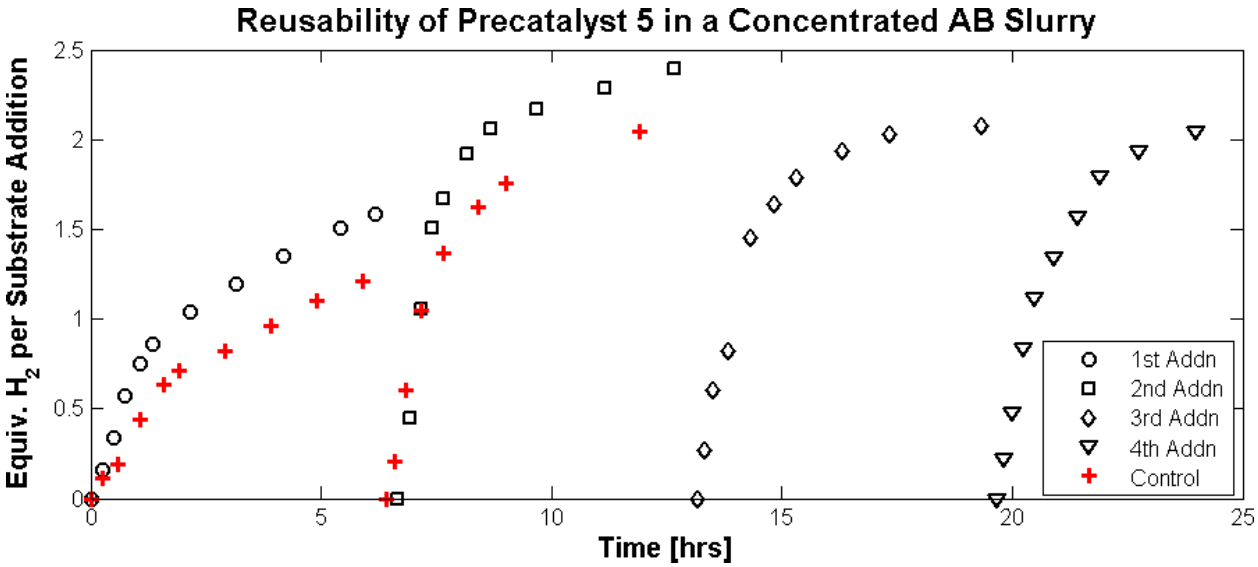

Figure S37—Multiple substrate additions to 0.1 mol % **5** in a *ca.* 16 M slurry of AB. The thermal control (identical conditions sans catalyst) is overlayed in red. Only a slight deviation between the catalyzed run and the control is observed. Notably, this system achieves 4.5 wt. % H_2 release. The similarity of the catalyzed and control experiments eliminates the ability to attribute dehydrogenation activity to **5** under these conditions.

Under concentrated AB conditions, little difference was observed between catalyzed and uncatalyzed experiments. This is attributable to thermal dehydrogenation processes dominating at high [AB]. With low catalyst loading (0.1 mol %), these conditions fail to lend insight into the role of the catalyst but

further optimization of the catalyzed systems for both precataylsts **4** and **5** is underway. Corroborating the concentration dependence of thermally induced, solution state AB dehydrogenation, rapid H_2 release is observed even after the first substrate addition under these more concentrated conditions. The increase from 1.5 equiv. to 2.0 equiv. released in control runs 1 and 2 is attributed to the presence of reactive dehydrogenation intermediates and improved stirring resulting from doubling the volume of diglyme. Presumably, solid-state thermal dehydrogenation is also playing a role in these slurry reactions.[16]

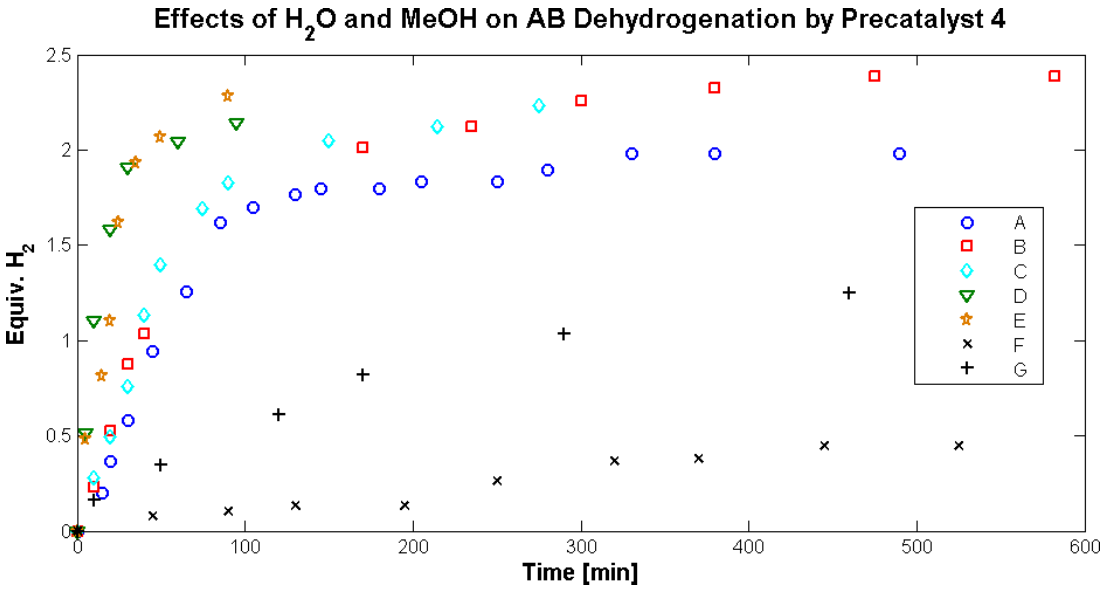

Figure S38—Hydrogen evolution profiles for reactions of precatalyst **4** with dry AB (A), AB and water (B-D), and AB and methanol (E). Control reactions with dry AB (F) and AB with water added (G) are included for comparison.

A significant disparity in the rate and extent of hydrogen evolution was observed when using sublimed AB (A) and unpurified AB (B). This rate increase was attributed to water, as sublimed AB that was later exposed to air showed a similar H_2 evolution profile to unpurified AB (C). Addition of 50 mol % H_2O to dehydrogenation experiements resulted in a significant rate increase, releasing over 2 equiv. of H_2 in 1 h (D). A similar effect was observed with the addition of 20 mol % methanol, again resulting in a significant increase to the rate and extent of dehydrogenation. Addition of 50 mol % H_2O to an AB solution lacking catalyst also leads to a greater extent of H_2 release (G). Though hydrolysis[17] and acid catalysis[17b,18] are established methods for the dehydrogenation of AB, the resulting B–O bonds likely preclude facile recyclability and therefore these systems were not studied further. Though little effect was observed for the source of AB utilized with precatalyst **5**, reported experiments use rigorously purified AB unless stated otherwise. Control experiments (with AB and **4**) were run on each batch of substrate to ensure consistency.

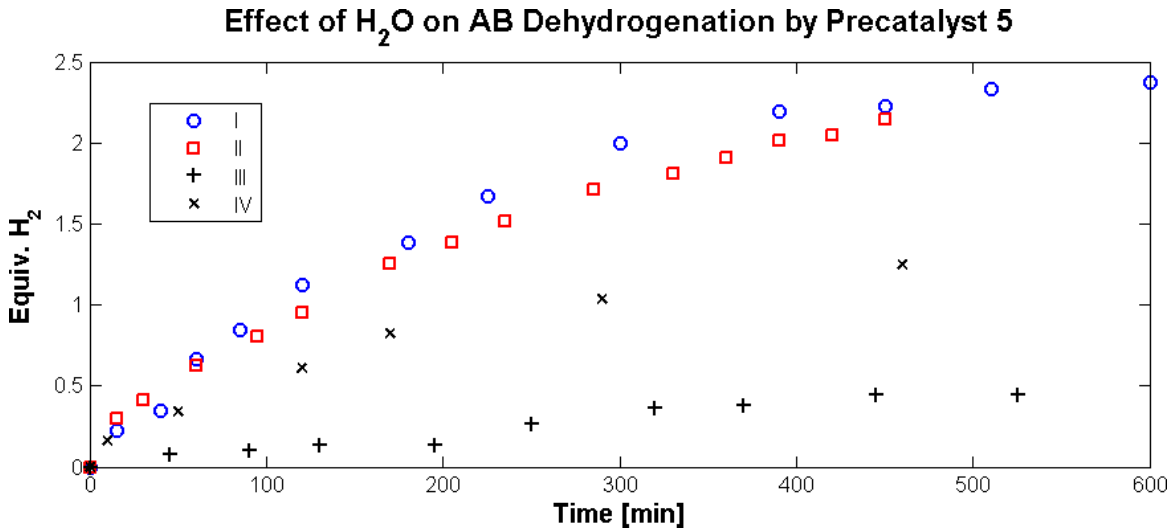

Figure S39—Hydrogen evolution profiles for reactions of precatalyst **5** with dry AB (I) and AB and water (II). Control reactions with dry AB (III) and AB with water added (IV) are included for comparison.

Table S1. Mo-Based Homogeneous Precatalysts for AB Dehydrogenation in Comparison to Precatalysts Reported to Release ≥2.0 equiv of H_2.

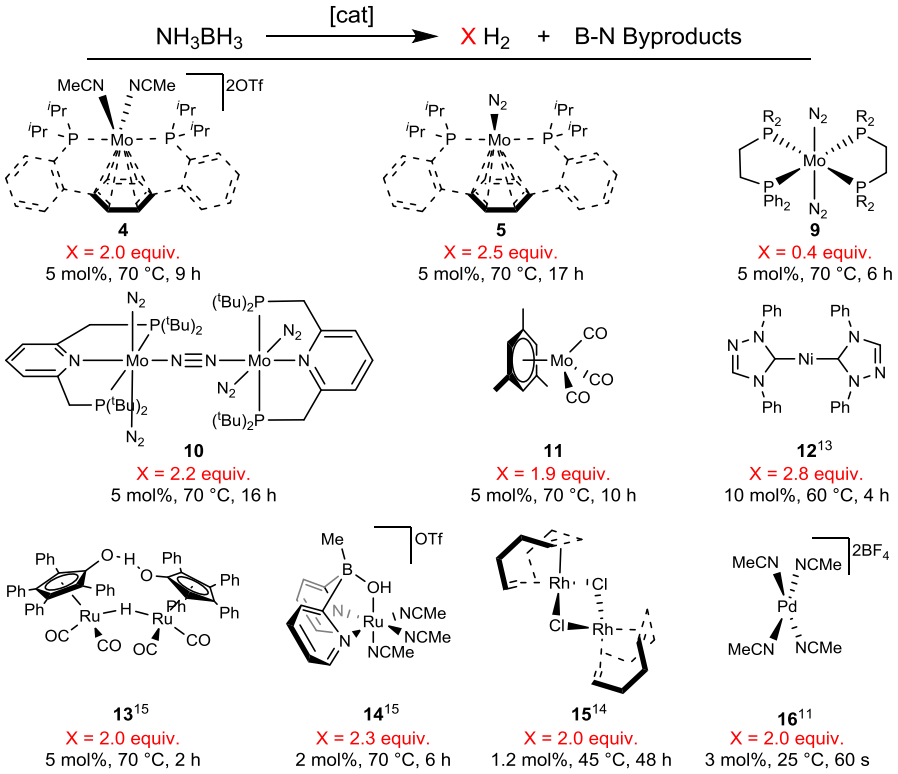

Kinetic Data

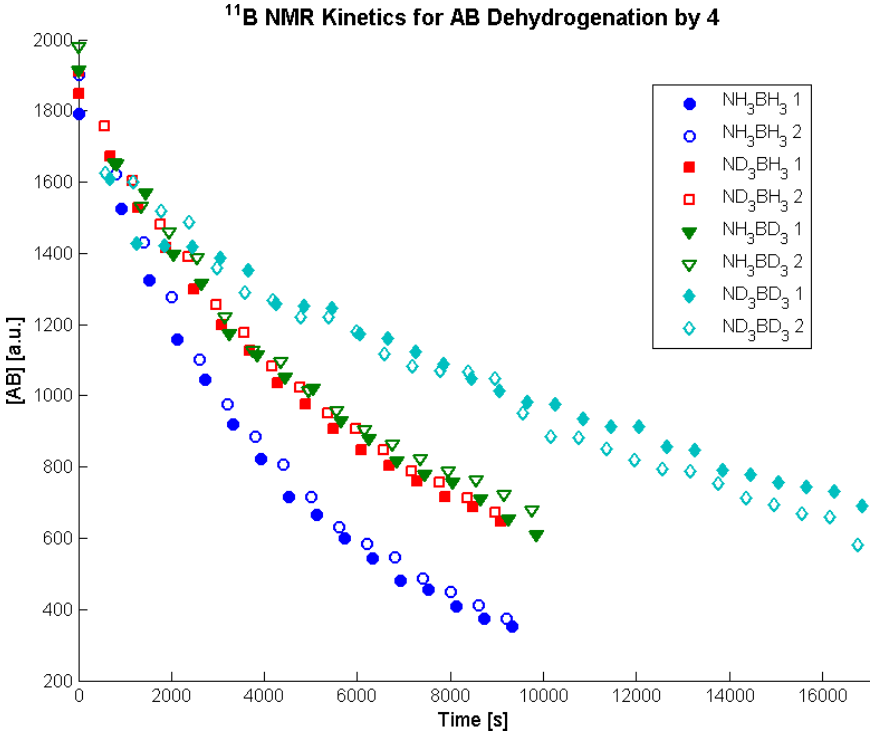

Figure S40—Relative concentration vs. time plots for reactions of AB isotopologs with catalytic **4** as monitored by ^{11}B NMR spectroscopy.

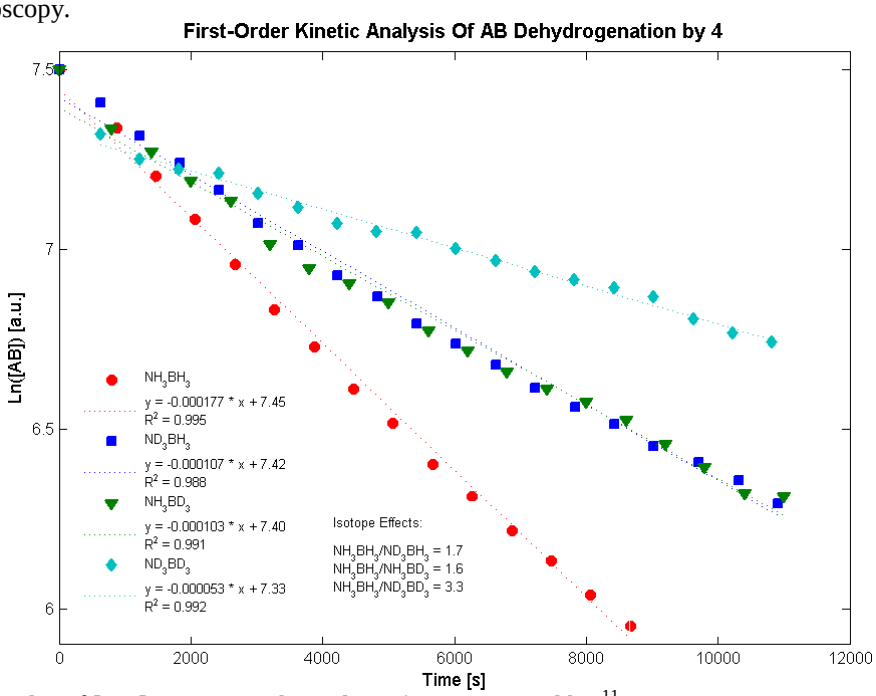

Figure S41—Log plot of [AB] vs. time with catalytic **4** as monitored by ^{11}B NMR spectroscopy. Isotope effects were calculated from the ratios of the respective slopes and are reported in the inset.

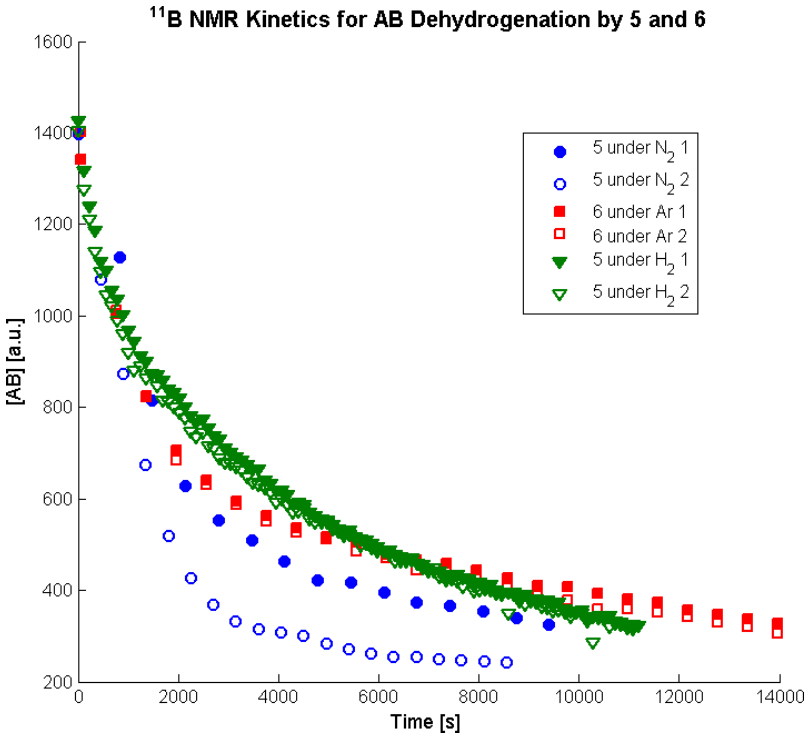

Figure S42—Relative concentration vs. time plots for reactions of AB with catalytic **5** and **6** as monitored by ^{11}B NMR spectroscopy.

Analysis of the dehydrogenation kinetics for **5** showed neither first- nor second-order behavior. The possibility of the equilibrium between **5** and **6** ([H_2] increases with time) affecting the rate of the reaction was ruled out via measuring kinetics from isolated **6** (red squares). Addition of 1 atm of H_2 to precatalyst **5** prior to heating demonstrated *pseudo*-first-order kinetics. This is consistent with product (H_2) inhibition, but further experimentation is required to confirm this hypothesis.

Crystallographic Information

CCDC deposition numbers 804890, 1008197, 1008330-1008331, and 1008356-1008357 contain the supplementary crystallographic data for this paper. These data can be obtained free of charge from The Cambridge Crystallographic Data Centre via www.ccdc.cam.ac.uk/data_request/cif.

Refinement Details—In each case, crystals were mounted on a glass fiber or nylon loop using Paratone oil, then placed on the diffractometer under a nitrogen stream. Low temperature (100 K) X-ray data were obtained on a Bruker APEXII CCD based diffractometer (Mo sealed X-ray tube, K_α = 0.71073 Å) or a Bruker SMART CCD based diffractometer (Mo sealed X-ray tube, K_α = 0.71073 Å). All diffractometer manipulations, including data collection, integration, and scaling were carried out using the Bruker APEXII software.[19] Absorption corrections were applied using SADABS.[20] Space groups were determined on the basis of systematic absences and intensity statistics and the structures were solved by direct methods using XS[21] or by intrinsic phasing using XT (incorporated into SHELXTL) and refined by full-matrix least squares on F^2. All non-hydrogen and hydride atoms were refined using anisotropic displacement parameters. Non-hydride hydrogen atoms were placed in the idealized positions and refined using a riding model. The structure was refined (weighed least squares refinement on F^2) to convergence. Graphical representation of structures with 50% probability thermal ellipsoids was generated using Diamond visualization software.[22]

Table S2. Crystal and refinement data for complexes **2-5** and **7-8**.

	2	**3**	**4**	**5**	**7**	**8**
CCDC Number[23]	804890	1008197	1008330	1008356	1008331	1008357
Empirical formula	$C_{33}H_{40}MoO_3P_2$	$C_{34}H_{40}F_6MoO_8P_2S_2$	$C_{36.67}H_{46}F_6MoN_{2.33}O_6P_2S_2$	$C_{30}H_{40}MoN_2P_2$	$C_{56}H_{64}BMoNP_2$	$C_{58}H_{71}BMoOP_2$
Formula weight	642.53	912.66	951.42	586.52	919.77	952.83
T (K)	100	100	100	100	100	100
a, Å	12.9284(7)	12.7866(6)	32.0444(10)	8.9892(3)	12.7883(6)	11.1314(5)
b, Å	12.6055(6)	16.4447(7)	32.0444(10)	23.8655(7)	16.1757(7)	17.1403(8)
c, Å	19.2797(9)	17.5292(7)	21.1665(9)	12.7797(4)	23.2443(10)	26.9594(12)
α, °	90	90	90	90	90	90
β, °	100.020(2)	91.785(2)	90	94.7145(16)	101.250(2)	94.544(2)
γ, °	90	90	120	90	90	90
Volume, Å^3	3094.1(3)	3684.1(3)	18822.7(14)	2732.37(15)	4715.9(4)	5127.6(4)
Z	4	4	18	4	4	4
Crystal system	Monoclinic	Monoclinic	Trigonal	Monoclinic	Monoclinic	Monoclinic
Space group	P $2_1/c$	P $2_1/n$	R3*c*	P $2_1/c$	P $2_1/c$	P $2_1/c$
d_{calc}, g/cm^3	1.379	1.645	1.511	1.426	1.295	1.234
θ range, °	2.44 to 30.54	1.698 to 45.424	2.059 to 43.500	1.707 to 45.535	1.544 to 39.298	1.409 to 45.385
μ, mm^{-1}	0.559	0.637	0.563	0.619	0.384	0.357
Abs. Correction	Semi-empirical	Semi-empirical	Semi-empirical	Semi-empirical	Semi-empirical	Semi-empirical
GOF	1.631	1.130	1.056	1.111	1.120	1.092
R_1 ,[a] wR_2 [b] [I>2 σ(I)]	0.0313, 0.0313	0.0464, 0.1251	0.0371, 0.0855	0.0493, 0.0951	0.0731, 0.1417	0.0448, 0.1007
Diffractometer	APEXII	APEXII	APEXII	SMART	APEXII	APEXII

[a] $R_1 = \sum||F_o| - |F_c||/\sum|F_o|$. [b] $wR_2 = [\sum[w(F_o^2-F_c^2)^2]/\sum[w(F_o^2)^2]]^{1/2}$.

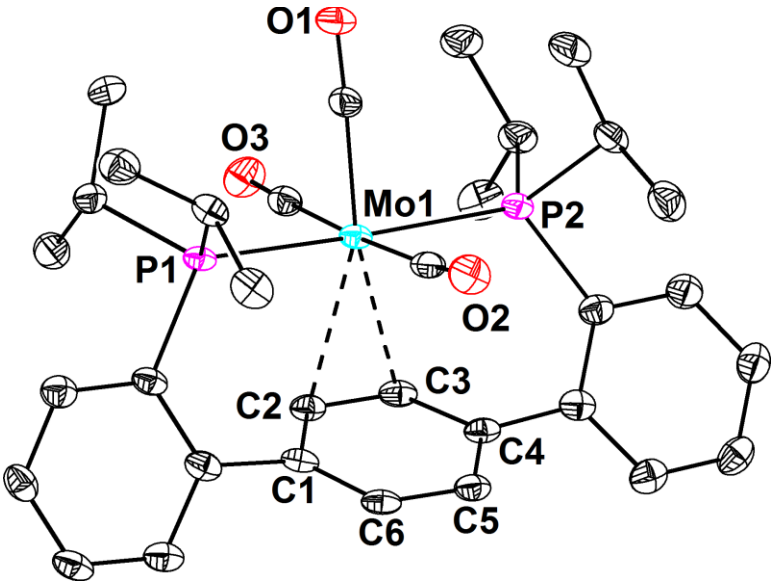

Figure S43—Structural drawing of **2** with 50% probability ellipsoids. Co-crystallized toluene and hydrogen atoms are omitted for clarity.

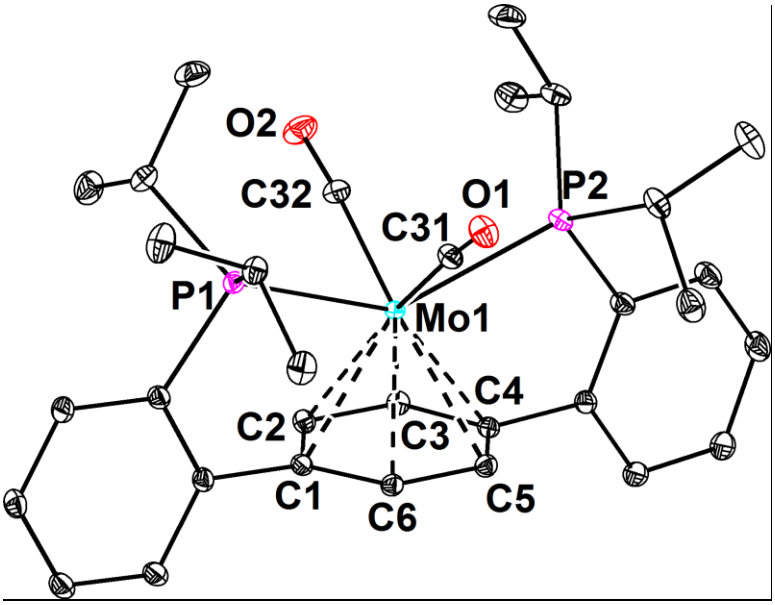

Figure S44— Structural drawing of **3** with 50% probability ellipsoids. Outer-sphere triflate ions and hydrogen atoms are omitted for clarity.

Special refinement details for 3— The crystal was twinned by a 180 degree rotation about the a axis.
An HKLF 5 file was generated with the TwinRotMat option in PLATON.
The twin ratio refined to 0.82:0.18.

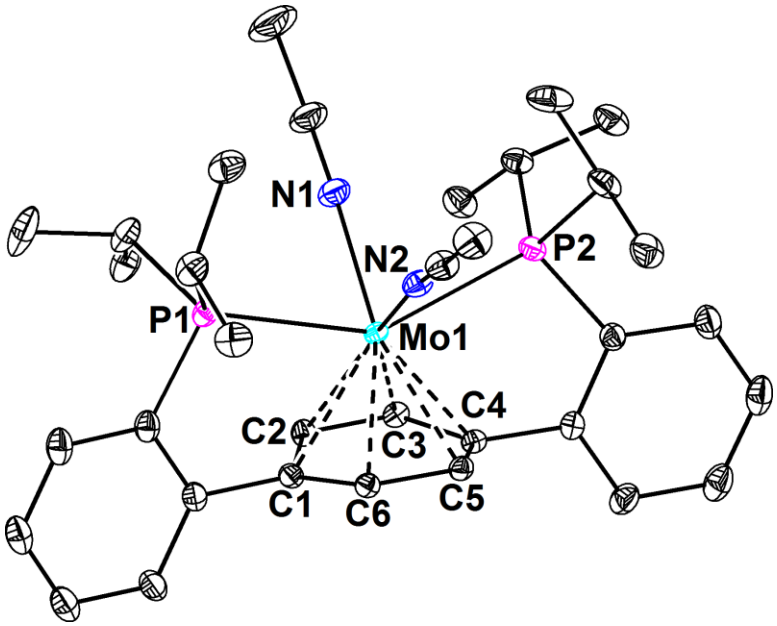

Figure S45— Structural drawing of **4** with 50% probability ellipsoids. Co-crystallized acetonitrile, outer-sphere triflate ions and hydrogen atoms are omitted for clarity.

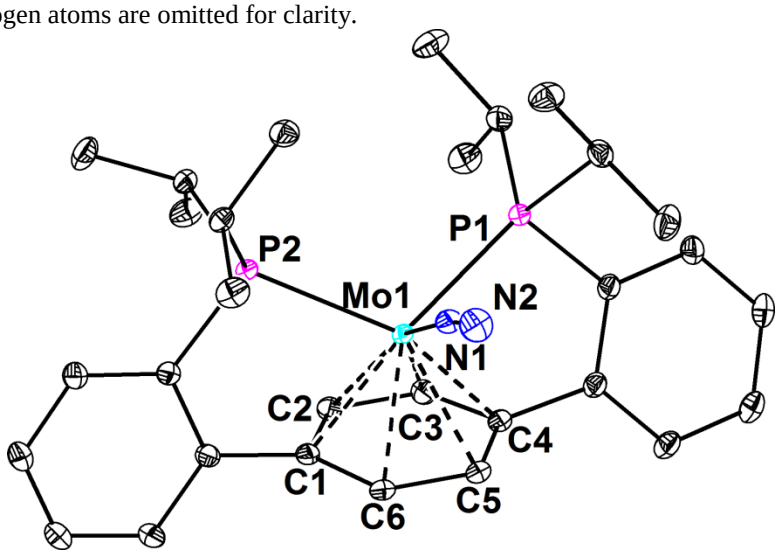

Figure S46—Structural drawing of **5** with 50% probability ellipsoids. Hydrogen atoms are omitted for clarity.

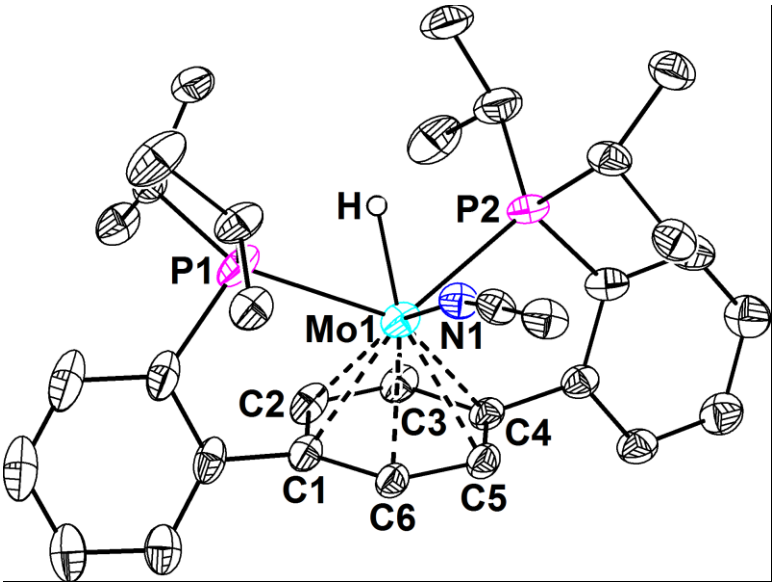

Figure S47—Structural drawing of **7** with 50% probability ellipsoids. Outer-sphere tetraphenylborate molecule and hydrogen atoms (except for the hydride) are excluded for clarity.

Special refinement details for 7—The ligand isopropyl groups were positionally disordered and satisfactorilly modeled as approximately a 70:30 mixture using "PART" cards in SHELX.

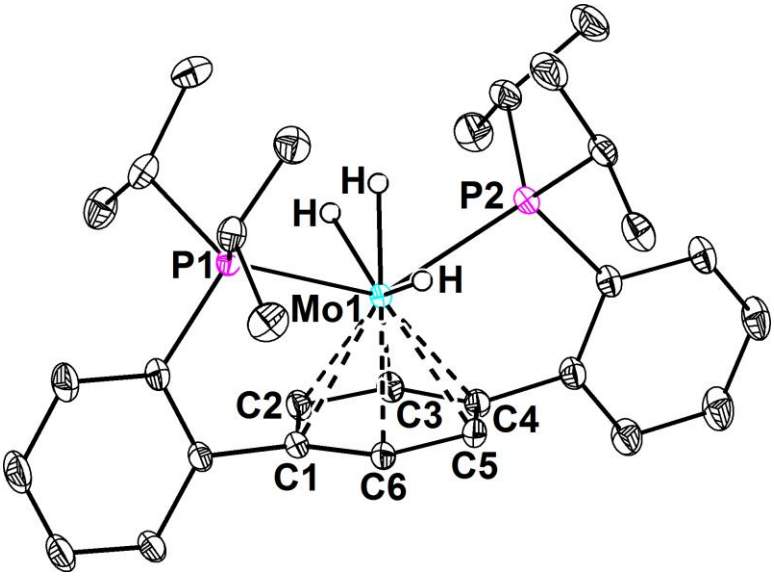

Figure S48—Structural drawing of **8** with 50% probability ellipsoids. A co-crystallized THF molecule and hydrogen atoms (except the hydrides) are omitted for clarity.

References

(1) Pangborn, A. B.; Giardello, M. A.; Grubbs, R. H.; Rosen, R. K.; Timmers, F. J. *Organometallics* **1996**, *15*, 1518.
(2) Velian, A.; Lin, S. B.; Miller, A. J. M.; Day, M. W.; Agapie, T. *J. Am. Chem. Soc.* **2010**, *132*, 6296.
(3) Tate, D. P.; Knipple, W. R.; Augl, J. M. *Inorg. Chem.* **1962**, *1*, 433.
(4) Archer, L. J.; George, T. A. *Inorg. Chem.* **1979**, *18*, 2079.
(5) Arashiba, K.; Miyake, Y.; Nishibayashi, Y. *Nat. Chem.* **2011**, *3*, 120.
(6) Pidcock, A.; Smith, J. D.; Taylor, B. W. *J. Chem. Soc. A.* **1967**, 872.
(7) Keaton, R. J.; Blacquiere, J. M.; Baker, R. T. *J. Am. Chem. Soc.* **2007**, *129*, 1844.

(8) Marziale, A. N.; Friedrich, A.; Klopsch, I.; Drees, M.; Celinski, V. R.; Guenne, J. S. A. D.; Schneider, S. *J. Am. Chem. Soc.* **2013**, *135*, 13342.
(9) Wender, I.; Friedel, R. A.; Orchin, M. *J. Am. Chem. Soc.* **1949**, *71*, 1140.
(10) Fulmer, G. R.; Miller, A. J. M.; Sherden, N. H.; Gottlieb, H. E.; Nudelman, A.; Stoltz, B. M.; Bercaw, J. E.; Goldberg, K. I. *Organometallics* **2010**, *29*, 2176.
(11) Conley, B. L.; Guess, D.; Williams, T. J. *J. Am. Chem. Soc.* **2011**, *133*, 14212.
(12) (a) Grundemann, S.; Limbach, H. H.; Buntkowsky, G.; Sabo-Etienne, S.; Chaudret, B. *J. Phys. Chem. A.* **1999**, *103*, 4752. (b) Gelabert, R.; Moreno, M.; Lluch, J. M.; Lledos, A.; Pons, V.; Heinekey, D. M. *J. Am. Chem. Soc.* **2004**, *126*, 8813.
(13) Janak, K. E.; Shin, J. H.; Parkin, G. *J. Am. Chem. Soc.* **2004**, *126*, 13054.
(14) (a) Wang, J. S.; Geanangel, R. A. *Inorg. Chim. Acta.* **1988**, *148*, 185. (b) Shaw, W. J.; Linehan, J. C.; Szymczak, N. K.; Heldebrant, D. J.; Yonker, C.; Camaioni, D. M.; Baker, R. T.; Autrey, T. *Angew. Chem. Int. Ed.* **2008**, *47*, 7493.
(15) Blaquiere, N.; Diallo-Garcia, S.; Gorelsky, S. I.; Black, D. A.; Fagnou, K. *J. Am. Chem. Soc.* **2008**, *130*, 14034.
(16) Baitalow, F.; Baumann, J.; Wolf, G.; Jaenicke-Rossler, K.; Leitner, G. *Thermochim Acta* **2002**, *391*, 159.
(17) (a) Chandra, M.; Xu, Q. *J Power Sources* **2006**, *156*, 190. (b) Stephens, F. H.; Pons, V.; Baker, R. T. *Dalton. Trans.* **2007**, 2613. (c) Diwan, M.; Diakov, V.; Shafirovich, E.; Varma, A. *Int. J. Hydrogen Energ.* **2008**, *33*, 1135. (d) Hamilton, C. W.; Baker, R. T.; Staubitz, A.; Manners, I. *Chem. Soc. Rev.* **2009**, *38*, 279.
(18) (a) Kelly, H. C.; Marchello, F. R.; Giusto, M. B. *Inorg. Chem.* **1964**, *3*, 431. (b) Kelly, H. C.; Marriott, V. B. *Inorg. Chem.* **1979**, *18*, 2875. (c) Stephens, F. H.; Baker, R. T.; Matus, M. H.; Grant, D. J.; Dixon, D. A. *Angew. Chem. Int. Ed.* **2007**, *46*, 746.
(19) APEX2, Version 2 User Manual, M86-E01078, Bruker Analytical X-ray Systems, Madison, WI, June 2006.
(20) Sheldrick, G.M. "SADABS (version 2008/1): Program for Absorption Correction for Data from Area Detector Frames", University of Göttingen, 2008.
(21) Sheldrick, G.M. (2008). Acta Cryst. A64, 112-122.
(22) Brandenburg, K. (1999). DIAMOND. Crystal Impact GbR, Bonn, Germany.
(23) Crystallographic data have been deposited at the CCDC, 12 Union Road, Cambridge CB2 1EZ, UK and copies can be otained on request, free of charge, by quoting the publication citation and the respective deposition numbers.